SIMULATION OF ATMOSPHERIC FLOWS IN SHORT WIND TUNNEL TEST SECTIONS

by

J. A. Peterka* and J. E. Cermak**

for

Center for Building Technology, IAT
National Bureau of Standards
Washington, D.C. 20234

Fluid Mechanics Program
Fluid Dynamics and Diffusion Laboratory
Department of Civil Engineering
Colorado State University
Fort Collins, Colorado
June, 1974

* Assistant Professor
** Professor-in-Charge, Fluid Mechanics Program

CER73-74JAP-JEC32

TABLE OF CONTENTS

ACKNOWLEDGMENTS

The support of the Center for Building Technology, Institute of Applied Technology of the National Bureau of Standards is gratefully acknowledged. Data acquisition was performed by Dr. S. K. Nayak and Mr. G. L. Marsh with support by Mr. A. C. Hansen.

LIST OF SYMBOLS

X,Y,Z	Wind Tunnel Coordinate System
Y_{ref}	Reference Height for Profile Nondimensionalization
Y_o	Effective Roughness Length
U	Local Mean Velocity
U_{ref}	Mean Velocity at Height Y_{ref}
U_{RMS}	Root-Mean-Square Velocity
$\overline{u'v'}$	Second Order Velocity Correlation
ΔX	Separation Distance for Velocity Correlations
X_o	Zero-Crossing for Autocorrelation Functions
$R(\Delta X)$	Normalized Longitudinal Velocity Space Correlation
L_x	Eulerian Integral Scale
n	Frequency in Hz
$F(n)$	Velocity Spectral Function
δ	Boundary Layer Thickness

I. INTRODUCTION

1.1 Scope of the Study

The design for wind effects on buildings has traditionally been performed in a highly empirical manner. However, within the last decade modeling techniques have been developed which permit the rational design of structures for wind resistance--Cermak (3,4) and Davenport et al. Recent design approaches rely on the availability of wind pressure information derived from measurements on small-scale models placed in an "appropriate" wind tunnel.

The realization that wind tunnels can be used as an effective tool in designing buildings against wind damage has caused considerable thought and effort to be directed toward determination of what constitutes an "appropriate" wind tunnel. A decade of research on turbulent boundary layers formed over rough surfaces in a long (30-40 m) test-section wind tunnel has demonstrated that a wind tunnel of this type is indeed satisfactory and "appropriate"--Cermak (4). Unfortunately, long test-section wind tunnels are costly to build and require large buildings for housing with the result that very few are now in existence--the major facilities are located at Colorado State University and the University of Western Ontario. On the other hand, many aeronautical wind tunnels (short test-section type) exist throughout the world at universities, government operated laboratories and industrial laboratories. Although considerable effort has been expended in adapting these short test-section wind tunnels to the modeling of atmospheric flows (Section 1.2), there is not a clear indication at this time that satisfactory simulation can be achieved. Jensen (15) has demonstrated that uniform flow or boundary-layer flows with the wrong turbulence

scale can lead to incorrect pressure distributions; therefore, the pressure data from short test-section wind tunnels must be viewed with caution. Development of a thick turbulent boundary layer in a short test-section wind tunnel requires initial stimulation of the boundary layer by some system of momentum sinks. Although devices such as graded screens, grids, vortex generators, spires, roughness plates, etc. have yielded reasonable vertical gradients of mean velocity, no definitive study has been made to determine how realistic are the resulting turbulence structures.

The purpose of this study was to develop an optimum system for generating thick turbulent boundary layers with a proper integral scale to simulate the atmospheric boundary layer in a short test-section wind tunnel. In particular, a system was to be developed which could be adapted to the 4 x 4 ft by 12 ft long test section of the University of the Philippines wind tunnel to study wind pressures on buildings resulting from typhoons.

1.2 Review of Previous Modeling Techniques

The need for wind tunnels to study atmospheric flow phenomena has prompted a number of investigators to convert existing short test-section wind tunnels or to build wind tunnels with test sections significantly shorter than required by a natural boundary layer development. Most of these have been reported rather recently, since 1968.

Methods of generating turbulent shear flow have been known for many years. Lawson (16) provided a review of those techniques and their possible use for atmospheric flow simulation. Cowdrey (12) showed a technique for designing horizontal rods to provide desired mean velocity profiles. Cockrell and Lee (5) used horizontal rods designed with

Cowdrey's technique and also used solid "mixing wedges" on the tunnel floor to simulate a neutrally stable atmospheric flow. Their technique required a fairly long test section (approximately 40 duct heights) before the boundary-layer settled down to an equilibrium condition.

An early use of vortex generators at the test section entrance to simulate atmospheric flows was reported by Armitt and Counihan (1). Their triangular wedge shape resulted in excessive organized longitudinal vorticity at their test station. Further development of the vortex generators with appropriate roughnesses has been performed by Counihan (7-11). His development has resulted in what he claims to be an acceptable simulation of a neutrally stable boundary-layer flow four and one-half boundary-layer heights downstream of the generators. Because he presented no data upstream or downstream from his measurement station, it is not possible to determine whether or not the boundary-layer was in a reasonable state of equilibrium. Triangular vortex generators were used by Sundaram et al. (22) in combination with a trip fence to demonstrate the technique of shortening the development length. Their limited data showed some promise of successful simulation.

The Canadian National Research Council has had a program to develop flow modeling in a short test section for several years. An early attempt, Templin (23), used a grid of horizontal bars with little success. Later attempts have used spires at the test section entrance. Standen et al. (20), Standen (21), and Wardlaw (26) described the technique and compared pressures measured on a structure with measurements in a conventional naturally developed boundary-layer and with field measurements. While the extent of comparison was not sufficiently extensive to demonstrate complete acceptability, the

technique did show promise. Approximately six boundary-layer heights were required to establish equilibrium. Some of their data indicated a possibility of undesirable organized vorticity in the outer portions of the boundary-layer. A spire-generated boundary-layer was also used by Dreher and Cermak (14) at Colorado State University. However, the mean velocity profile showed distortions characteristic of too small a surface-roughness height.

Two investigators have used a coarse grid covering the entire cross section combined with a two-dimensional barrier fence across the floor either upstream or downstream of the grid. Barrett (2) used an upstream barrier with grid to develop the boundary layer and to even out nonuniformities from a high-angle diffuser a short distance upstream. Significant nonuniformities in the approach flow did not permit a good evaluation of the boundary-layer-generation technique. Cook (6), using a barrier downstream of his grid developed a boundary layer simulating the lower one-third of the atmospheric boundary layer with a realistic integral scale. However, his roughness elements were spaced sufficiently closely that a large effective wall displacement occurred.

Fluid barriers or trips have been used by several investigators. Teunissen (24,25) used an array of jets pointing in the direction of the main flow to provide turbulence structure and mean velocity defect to simulate atmospheric flow in an 8 x 8 inch duct. He found it necessary to include a two-dimensional solid fence to trip the flow and carefully selected floor roughness to properly simulate an atmospheric flow. The simulation was very encouraging; however, scale-up to a facility large enough to accomodate a model at 1:200 to 1:400 has not yet been demonstrated. Schon and Mery (19) used a jet blowing perpendicular to

the main flow at the leading edge to thicken their boundary layer. They were limited in the thickness of the boundary layer they could develop by this technique. Morkovin et al. (17) used a row of counter-jets at floor level directed upstream at various angles to the flow. They did not measure sufficient turbulence properties to indicate acceptability of their simulation. Nee (18) has recently completed a wind tunnel which will use lateral jets to control the flow properties.

II. WIND SIMULATION FACILITIES

2.1 Wind Tunnel

The study was performed in the Industrial Aerodynamics Wind Tunnel at Colorado State University (Fig. 1). The test section is 6 x 6 ft in cross section with a length of 36.5 ft and contraction ratio of 4:1. An axial-flow blower driven by a 75 hp constant speed motor provides wind velocities up to 65 ft/sec. Continuous variation of wind speed is accomplished by varying the fan blade pitch.

2.2 Spire and Roughness Arrays

The intent of the study was to determine a combination of disturbance devices and roughnesses to simulate a neutral atmospheric flow for two classes of roughness defined by mean velocity power-law exponents in the ranges 0.14-0.20 and 0.28-0.35. A location 18 ft downstream in the test section was selected as the cross section at which the boundary-layer simulation would be targeted. This location was scaled to the end of the 12 ft test section of the University of the Philippines wind tunnel. In order to provide a flow in which models as large as 1:50 could be used, as deep a boundary layer as possible was desired, even to the point of modeling only the lower portion of the atmospheric boundary layer.

With the present status of expertise in generating artificially stimulated boundary layers outlined in Section 1.2, spires with a roughened floor were selected as the most likely means of obtaining an acceptable simulation. Spires used in a previous study (14) provided a starting point for spire geometry. A number of spire geometries and roughness heights were tried. Two combinations of spires and roughness

were found which met the power law velocity-exponent criteria. The spire and roughness array geometries are shown in Fig. 2. Configuration 1 yielded a profile in the 0.28-0.35 range while Configuration 2 provided a profile close to the 0.14-0.20 range. Photographs of Configurations 1 and 2 are shown in Fig. 3.

2.3 Instrumentation and Data Acquisition

During the initial stages where spire and roughnesses were selected, most mean velocity profiles were obtained with a pitot tube with pressure differences measured with an MKS Baratron pressure transducer. For final data (including all data presented in this report), velocity data was taken by hot-wire anemometer. Data associated with Configuration 1 was taken with a Thermosystems Model 1054B constant temperature anemometer on loan from National Bureau of Standards for checkout purposes. The remainder of the data was taken with a DISA model 55D01 constant temperature anemometer.

Autocorrelations, space correlations and spectra were obtained for selected locations. Autocorrelations for Configuration 1 were obtained using a Saicor Model SAI-43A Correlation and Probability Analyzer which was on loan from National Bureau of Standards for checkout. The remaining correlations were obtained on a Princeton Correlator. Spectra were obtained by Fourier transform of the correlations. Each correlation was digitized at two millisecond intervals (300-350 points per correlation) and transformed by a Fast-Fourier-Transform algorithm on the CSU CDC 6400 computer.

Six measurement stations were defined in the wind tunnel, two each at three downstream positions. The three longitudinal positions were at X=14, 18 and 28 ft from the spires at the test-section entrance

(see Fig. 2 for coordinate system). At each of these distances, measurement stations were located on the centerline of the wind tunnel and 1/2 spire spacing off the centerline. At each of these six stations, data was taken along a vertical line. Mean velocity and turbulence data were taken at all stations on a vertical traverse spanning the entire boundary-layer thickness. Correlations and spectra were taken at selected locations chosen to show certain features of the turbulent structure.

III. RESULTS

3.1 Mean Velocity

The mean velocity profiles for the two desired power law exponent flows are shown in Fig. 4. The data is nondimensionalized with respect to the velocity U_{ref} measured at a height Y_{ref}. These reference values are not intended to represent the edge of the simulated boundary layer flow but a convenient position for nondimensionalization. The best value to use for the simulated boundary-layer thickness will depend on the scale of models to be placed in the flow. This scale should not be selected until the turbulent properties of the flow have been examined. A value of Y_{ref} of 52 inches was selected to nondimensionalize all data since all mean velocity profiles measured obeyed a power law to that height. Some profiles had a power law profile to a height of as much as 58 inches before effects of the ceiling boundary layer were felt. The solid lines in Fig. 4 represent a least squares fit of the data to a power-law velocity profile. The exponents were found to be 0.312 and 0.138.

An important criterion in the simulation of atmospheric flows is the effective roughness length. Significant difficulties were encountered in this study in that excessively large values tended to occur. This difficulty was also evident in several of the reviewed publications. The final solutions for the present simulation represent reasonably acceptable values. Logarithmic plots of the data from Fig. 4 are shown in Fig. 5. As expected, a large portion of the boundary layer followed a logarithmic relationship. Roughness lengths Y_o determined from the graph are 0.884 inches for Configuration 1 (n=0.312) and Y_o=0.01 inches for Configuration 2 (n=0.138). The corresponding

prototype roughness lengths range from 22 to 88 inches for model scales of 1:25 to 1:100 for Configuration 1 and from 0.25 to 1.0 inches for Configuration 2. These values fall within the range of field values expected for the power law profiles given.

One of the greatest difficulties in developing a boundary layer with artificial stimulation has been that of generating a flow which is in equilibrium. Only the spire configuration used by the National Research Council (20, 21) and the multiple jet facility reported by Teunissen (25) have demonstrated some measure of equilibrium. The Canadian study required six spire heights to establish equilibrium--a condition which, for this study with a short test-section length available, would limit spires (and consequently boundary layer height) to less than half the wind tunnel height. Teunissen had such a small range of frequencies between the peak of his spectrum and viscous dissipation that his boundary layer reached equilibrium more quickly--about 4½ tunnel heights downstream. The desire for equilibrium in three tunnel heights ($4.1\ Y_{ref}$) in the present study represents a severe requirement. A necessary (but not sufficient) condition for equilibrium is a mean velocity profile invarient with longitudinal position. Figure 6 shows the mean velocity profiles for the three longitudinal measurement positions for both Configurations 1 and 2, plotted on log-log scales to show the power law relationship of the profiles. The solid lines are least square fits for the exponent n. The variation in exponent for Configuration 1 was from 0.336 to 0.245 from X=14 ft to X=28 ft. While the variation was not exceedingly large, equilibrium has certainly not been indicated in the strictest sense. The profiles for Configuration 2 show a variation with downstream extent sufficiently small to indicate the possibility of a fully developed flow.

An equilibrium boundary layer maintains itself by balancing the production of turbulence which is influenced by the roughness with the dissipation of that turbulent energy in viscous effects. The decay in exponent for Configuration 1 indicates that, for the given roughness, the boundary layer was seeking an exponent lower than those shown in Fig. 5 as it approached closer to equilibrium. It also indicates that larger roughness elements would be required in the region from X=14 to 28 ft to maintain an exponent in the range of 0.28-0.35 desired for a solution in Configuration 1. However, it was found that, for a particular spire, the roughness required to force a power-law variation in mean velocity was fixed--that is, one is not free to arbitrarily select a roughness to vary the exponent. A particular spire demands a particular roughness to obtain a power-law variation in mean velocity and together they define an exponent which may vary with downwind position. This need for a particular roughness has been noted before and was most clearly shown by Standen (21). His profiles showed two distinct power-law regions with incorrect roughness leading to the concept that the spires controlled the profile shape in the outer region of the boundary layer and the roughness controlled the profile shape in the inner portions. This concept, however, oversimplifies the mechanism. The roughness actually affects the profile over the entire height as is demonstrated in Fig. 7. Four mean velocity profiles are shown representing the solution profile for Configuration 1 and three alternate roughness heights. The data shows that the effects of spires and roughness interact so strongly that they must be considered together in their effect on the flow. This makes the design of a spire and roughness array to obtain a particular result (say a desired power-law exponent) a difficult task since one cannot, for

example, determine the effect of varying spire width without also trying a series of roughnesses with each spire width. It is thus not evident from the data shown in Figs. 4 and 5 what variations in spires and roughness would result in a mean velocity profile more stable in longitudinal variation than the data for Configuration 1.

It was found during the early testing that the spires followed by a roughness of uniform height did not produce a power law profile at the X=18 ft measurement station as readily as a roughness which was higher near the spires than farther down the test section. The effect of the roughness height gradation used for Configuration 1 appears to have the same effects as the barriers used previously by a number of investigators (2, 6, 7-11, 22, 25).

One concern resulting from the use of spires was the spanwise variation of flow properties. Figure 8 shows the comparison of the centerline mean velocity profile with the profile located 1/2 the spire span laterally from the centerline. Data is shown for Configurations 1 and 2 for all three longitudinal measuring stations. The agreement is generally within the measurement tolerance and no indication of a wake effect is evident in the mean velocity profiles. A more stringent test of lateral uniformity is the comparison of turbulence intensity profiles discussed in the next section.

3.2 Turbulence Intensity and Shear Stress

Turbulence intensity profiles showing longitudinal variation on the tunnel centerline for Configuration 1 are shown in Fig. 9. The vertical distance has been scaled by the distance Y_{ref} as was done for the mean velocity profiles. The magnitude of turbulence intensity is realistic for simulation of an atmospheric boundary layer. The decay

of intensity with longitudinal position is consistent with the decay of exponent noted above and provides further evidence that the flow was not in equilibrium but was seeking a profile of lower power-law exponent and lower turbulence intensity than was reached by 28 ft downstream. Figure 10 shows the lateral variation at the three measurement stations. Since turbulence decays at a slower rate than velocity defect in a wake flow, these profiles should be more sensitive to any remaining wake effects of the individual spires than the mean velocity profiles. An acceptable lateral uniformity is thus indicated for all three stations.

Longitudinal variation of turbulence intensity for Configuration 2 is shown in Fig. 11. The indication from the mean velocity profiles (Fig. 6) was that little or no change in profile shape was occurring with downstream position. The turbulence profiles, however, show a steady decay of turbulence intensity indicating that the boundary layer was not in equilibrium. Within the range of X=14 to 18 ft, the turbulence variation was small and could represent a flow sufficiently close to equilibrium for many measurement purposes. The overall level of turbulence intensity was somewhat below that expected for an atmospheric flow with the same power-law exponent. Figure 12 shows the lateral variation at all three measurement stations. The uniformity is acceptable.

Figure 13 demonstrates the absolute magnitude of the turbulence by referencing the rms velocity to the constant velocity U_{ref} at height Y_{ref}. Configuration 1 has a turbulent intensity approximately constant up to about 1/3 of the Y_{ref} height. Configuration 2 shows a roughly constant, but smaller, value to approximately 1/4 Y_{ref}.

Shear stress profiles for Configuration 1 are shown in Fig. 14. Both variation with longitudinal position and lateral displacement are shown. Good lateral uniformity is demonstrated but is to be expected from the turbulent intensity results. The lateral uniformity results are a good measure of the precision of the measurements. A steady decay of shear stress magnitude is shown with increasing longitudinal distance. This variation reflects the decay shown in power law exponent and turbulent intensity discussed above. It is difficult to define a region of solidly constant shear stress, but the region from the top of the roughness elements to about 1/3 of the Y_{ref} height could be considered to be a region of reasonably constant stress.

Shear stress results for Configuration 2 are shown in Fig. 15. The lateral uniformity again is good. Decay of shear stress with longitudinal position is consistent with the turbulent intensity results and confirms that the boundary layer was not in equilibrium in the longitudinal range considered.

3.3 Correlations, Integral Scales and Spectra

Longitudinal velocity correlations were taken at several heights above the wind-tunnel floor at all three measurement stations for both spire and roughness configurations. In addition, several correlations were taken at locations laterally spaced from the centerline to check for possible nonuniformities. Two correlations obtained at X=18', Y=13" on the centerline for Configuration 1 are shown in Fig. 16. The curves are in the form of a normalized longitudinal space correlation and are typical of all correlations measured. The solid line was obtained by an autocorrelation of a single hot wire and using Taylor's hypothesis $(\frac{\partial}{\partial t} = V \frac{\partial}{\partial x})$ to convert to a space frame. The correlation

has an unusual feature: a long negative tail extending past 100 inches (or about 1/2 second in time). When integral scales were computed from this and other correlation curves by the formula

$$L_X = \int_0^\infty R(\Delta X)\, d\Delta X \quad , \tag{1}$$

it was found that the positive area was nearly balanced by the negative area causing the calculated integral scale to be unrealistically small, and in some cases negative. Since the use of formula 1 to obtain integral scales from an autocorrelation requires that Taylor's hypothesis is valid, a check of the validity of that hypothesis was made by obtaining the correlation of physically spaced hot wires. The results of that investigation are shown in Fig. 16 as circles. The larger the distance that the circles fall below the solid curve, the less is the accuracy of the hypothesis. The reasonable agreement shown is an indication that, while not precisely correct for this flow, the hypothesis is acceptable for the computation of integral scales. It is possible that the long negative tail of the correlation is, in fact, due to the already demonstrated lack of equilibrium in the flow. All correlations measured showed this same characteristic tail although those from Configuration 2 were not as long.

Integral scales were finally obtained by use of the formula

$$L_X = \int_0^{X_o} R(\Delta X)\, d\Delta X \tag{2}$$

where X_o is the first zero crossing of the correlation function. This provides an estimate of the integral scale which should be fairly close to the correct value. The error in an estimate of this type should be such that the scale is slightly overestimated. This calculation

procedure is rather common, especially for atmospheric measurements, so that the values obtained should be useful for comparison of the boundary layer with atmospheric flow. The variation of integral scale with height and longitudinal position in the boundary layer for both configurations is shown in Fig. 17. The scale increases with height--as in the atmosphere--over the lower portion of the boundary layer but decreases again at larger heights. This decrease with height above the lower levels is a characteristic of most wind-tunnel simulations with a short test-section. The absolute magnitude of the integral scale compared to the atmosphere must be considered with the scale of the model to be employed. This will be discussed in Chapter IV.

The variation of integral scale with longitudinal position is shown in Fig. 17 at a constant elevation. Since the height chosen was near the peak scale for both configurations and because the tunnel boundary-layer thickness varied little with downstream distance, the trend of the integral scale is an indication of real development within the boundary layer. Again the indication is that, within the test region investigated, the boundary layer was seeking but had not quite attained, an equilibrium condition.

A longitudinal velocity spectrum is shown in dimensional form in Fig. 18a. The location is at 18 ft downstream and at 25 percent of the reference height for Configuration 1 at a point where the integral scale is still increasing with height. The important feature is the slope of the curve in the inertial subrange. A slope of -1.46 was obtained which is significantly different from -1.67 slope expected from a turbulence in equilibrium. A comparison of the spectra for several locations in the flow for both configurations is shown in Fig. 18b to

illustrate the vertical and longitudinal variations. It can be observed that the slopes, in general, tend to approach closer to the -1.67 value with increased longitudinal position and decreased turbulence intensity. This data further confirms statements made above relative to the equilibrium of the flow.

Figure 19 shows the velocity spectrum of Fig. 18a in nondimensionalized form. The location of the peak in amplitude and position in the frequencly domain was similar for the other spectra. The slope in the decay region was also similar although, as noted above, the slopes tended to be steeper for some situations. The frequency scale is commonly nondimensionalized in the form nL/U where L is some characteristic length such as the integral scale and U is the velocity at the elevation of interest. Since these values are related to the scale of the model involved, a discussion of the location of the peak referenced to these variables will be delayed until Chapter IV.

IV. CONCLUSIONS

Wind-tunnel simulations of atmospheric boundary-layer flow were obtained for two power law exponents at a station located three tunnel heights downstream of the test-section entrance with a 6 x 6 ft cross section wind tunnel. Spires extending the full height of the test section and appropriate roughness were used to generate a 52 inch deep boundary layer. Mean velocity profiles followed power-law relationships over virtually the entire height. Turbulence intensities were reasonable for the case with $\alpha=0.3$ but slightly low for the case with $\alpha=0.14$. Shear stress profiles were within an acceptable range although the depth of the roughly constant stress layer was not as large as might be desired.

The equilibrium of the boundary layers was examined using mean velocity, turbulence and shear stress profiles, integral scales and velocity spectra. The indications were that the boundary layers were not in equilibrium as far downstream as 4.7 wind-tunnel heights. Sufficient evidence is not presently available to demonstrate whether or not the flows were sufficiently close to equilibrium that errors in measurements on or about a model placed in the flows would be acceptably small. It is likely that such errors would be reasonably small.

The size of model which could be tested in the boundary layers generated in this study can be determined by examining the integral scales, the peak of the nondimensional spectra and the effective roughness length. Integral scales in the atmosphere generally run from about 400 to 700 ft. However, in typhoons the scales can be in the neighborhood of 200 ft. Using 200 ft as a reasonable target for wind

simulation tests which would be of interest for the Philippines area, the 0.4 and 0.6 ft scales measured in the two boundary layers give model scales of 1:300 to 1:500, say 1:400 as an average. Using an atmospheric boundary-layer thickness of 1000 and 1600 ft for the cases $\delta = 0.14$ and 0.30. The wind tunnel boundary-layer thickness for this scale would be $Y_L = 2.5$ ft and 4.0 ft--within the depth established for the two boundary layers.

Nondimensionalization of the velocity spectrum frequency scale by the term $n\delta/U$ tends to collapse atmospheric data to a single curve (23). The factor δ represents the atmospheric boundary-layer thickness. The peak of the spectra occur at $n\delta/U = 0.35$ with the ordinate in the form $nF(n)/U_{rms}^2$. Applying this criteria to the wind tunnel flows where the peak in the spectrum occurred at $n = 2$ (Fig. 19), values of δ were calculated to be 3.8 ft and 5.0 ft for Configuration 1 and 2 respectively. Assuming full scale values of δ of 1200 ft and 900 ft for the two power law profiles leads to wind tunnel scales of 1:300 for Configuration 1 and 1:180 for Configuration 2.

At scales of 1:300 and 1:180, the effective roughness lengths of .884 inches and 0.01 inches for $\alpha = 0.3$ and 0.14 respectively are 22 ft and .15 ft in the prototype. The value for Configuration 1 is large by a factor of three or more. While a zero-plane displacement could be used to reduce the roughness length, it involves a rather arbitrary assignment of a displacement which would not improve either the logarithmic or power-law description of the mean velocity profile. At scales of 1:300 and 1:180 the integral scales for the prototype become 180 ft and 72 ft for Configurations 1 and 2. These are somewhat small.

REFERENCES

1. Armitt, J. and J. Counihan, THE SIMULATION OF THE ATMOSPHERIC BOUNDARY LAYER IN A WIND TUNNEL, Atmospheric Environment, Vol. 2, pp. 49-71, 1968.

2. Barrett, R. V., A VERSATILE COMPACT WIND TUNNEL FOR INDUSTRIAL AERODYNAMICS, Technical Note, Atmospheric Environment, Vol. 6, pp. 491-498, 1972.

3. Cermak, J. E., V. A. Sandborn, E. J. Plate, G. H. Binder, H. Chuang, R. N. Meroney and S. Ito, SIMULATION OF ATMOSPHERIC MOTION BY WIND TUNNEL FLOWS, Report CER66JEC-VAS-EJP-GJB-HC-RNM-SI17, Fluid Mechanics Program, Colorado State Univ., 1966.

4. Cermak, J. E., LABORATORY SIMULATION OF THE ATMOSPHERIC BOUNDARY LAYER, AIAA J1, Vol. 9, pp. 1746-1754, 1971.

5. Cockrell, D. J. and B. E. Lee, METHODS AND CONSEQUENCES OF ATMOSPHERIC BOUNDARY LAYER SIMULATION, Paper 13-AGARD Conference Proc. No. 48 on Aerodynamics of Atmospheric Shear Flows, Munich, 1969.

6. Cook, N. J., ON SIMULATING THE LOWER THIRD OF THE URBAN ADIABATIC BOUNDARY LAYER IN A WIND TUNNEL, Atmospheric Environment, Vol. 7, pp. 691-705, 1973.

7. Counihan, J., AN IMPROVED METHOD OF SIMULATING AN ATMOSPHERIC BOUNDARY LAYER IN A WIND TUNNEL, Atmospheric Environment, Vol. 3, pp. 197-214, 1969.

8. Counihan, J., A METHOD OF SIMULATING A NEUTRAL ATMOSPHERIC BOUNDARY LAYER IN A WIND TUNNEL, Paper 14-AGARD Conference Proc. No. 48 on Aerodynamics of Atmospheric Shear Flows, Munich, 1969.

9. Counihan, J., FURTHER MEASUREMENTS IN A SIMULATED ATMOSPHERIC BOUNDARY LAYER, Atmospheric Environment, Vol. 4, pp. 259-275, 1970.

10. Counihan, J., WIND TUNNEL DETERMINATION OF THE ROUGHNESS LENGTH AS A FUNCTION OF THE FETCH AND THE ROUGHNESS DENSITY OF THREE-DIMENSIONAL ROUGHNESS ELEMENTS, Atmospheric Environment, Vol. 5, pp. 637-642, 1971.

11. Counihan, J., SIMULATION OF AN ADIABATIC URBAN BOUNDARY LAYER IN A WIND TUNNEL, Atmospheric Environment, Vol. 7, pp. 673-689, 1973.

12. Cowdrey, C. F., TWO TOPICS OF INTEREST IN EXPERIMENTAL INDUSTRIAL AERODYNAMICS, Symposium on Wind Effects on Buildings and Structures, National Physical Laboratory, Teddington, 1968.

13. Davenport, A. G. and N. Isyumov, THE APPLICATION OF THE BOUNDARY LAYER WIND TUNNEL TO THE PREDICTION OF WIND LOADING, Proc. International Research Seminar on Wind Effects on Buildings and Structures, Vol. 1, National Research Council, Canada, 1967.

14. Dreher, K. J. and J. E. Cermak, WIND LOADS ON A HOUSE ROOF, Report CER72-73KJD-JEC22, Fluid Mechanics Program, 1973.

15. Jensen, M., THE MODEL-LAW FOR PHENOMENA IN A NATURAL WIND, Ingenioren (International Edition), Vol. 2, pp. 121-128, 1958.

16. Lawson, T. V., METHODS OF PRODUCING VELOCITY PROFILES IN WIND TUNNELS, Research Note, Atmospheric Environment, Vol. 2, pp. 73-76, 1968.

17. Morkovin, M. V., H. M. Nagib and J. T. Yung, ON MODELING OF ATMOSPHERIC SURFACE LAYERS BY THE COUNTER-JET TECHNIQUE--PRELIMINARY RESULTS, Report AFOSR-TR-73-0592, Illinois Institute of Technology, 1972.

18. Nee, V. W., C. Dietrick, R. Betchov and A. A. Szewczyk, THE SIMULATION OF THE ATMOSPHERIC SURFACE LAYER WITH VOLUMETRIC FLOW CONTROL, Realism in Environmental Protection and Control, Proc. 19th Annual Tech. Meeting, Institute of Environmental Science, Anaheim, Calif., pp. 483-487, 1973.

19. Schon, J. P. and P. Mery, A PRELIMINARY STUDY OF THE SIMULATION OF NEUTRAL ATMOSPHERIC BOUNDARY LAYER USING AIR INJECTION IN A WIND TUNNEL, Atmospheric Environment, Vol. 5, pp. 299-311, 1971.

20. Standen, N. M., W. A. Dalgliesh and R. J. Templin, A WIND TUNNEL AND FULL-SCALE STUDY OF TURBULENT WIND PRESSURES ON A TALL BUILDING, Proc. Third International Conference on Wind Effects on Buildings and Structures, Tokyo, Japan, 1971.

21. Standen, N. M., A SPIRE ARRAY FOR GENERATING THICK TURBULENT SHEAR LAYERS FOR NATURAL WIND SIMULATION IN WIND TUNNELS, Report LTR-LA-94, National Aeronautical Establishment, Ottawa, Canada, 1972.

22. Sundaram, T. R., G. R. Ludwig and G. T. Skinner, MODELING OF THE TURBULENCE STRUCTURE OF THE ATMOSPHERIC SURFACE LAYER, AIAA J1, Vol. 10, pp. 743-750, 1972.

23. Templin, R. J., INTERIM PROGRESS NOTE ON SIMULATION OF EARTH'S SURFACE WINDS BY ARTIFICIALLY THICKENED WIND TUNNEL BOUNDARY LAYERS, Report LTR-LA-22, National Aeronautical Establishment, Ottawa, Canada, 1969.

24. Teunissen, H. W., AN INJECTOR-DRIVEN WIND TUNNEL FOR THE GENERATION OF TURBULENT FLOWS WITH ARBITRARY MEAN VELOCITY PROFILE, Tech. Note 133, University of Toronto Institute for Aerospace Studies, Toronto, 1969.

25. Teunissen, H. W., SIMULATION OF THE PLANETARY BOUNDARY LAYER IN A MULTIPLE-JET WIND TUNNEL, Report 182, University of Toronto Institute for Aerospace Studies, Toronto, 1972.

26. Wardlaw, R. L., WIND TUNNEL INVESTIGATIONS IN INDUSTRIAL AERODYNAMICS, Canadian Aeronautics and Space Journal, Vol. 18, pp. 53-59, 1972.

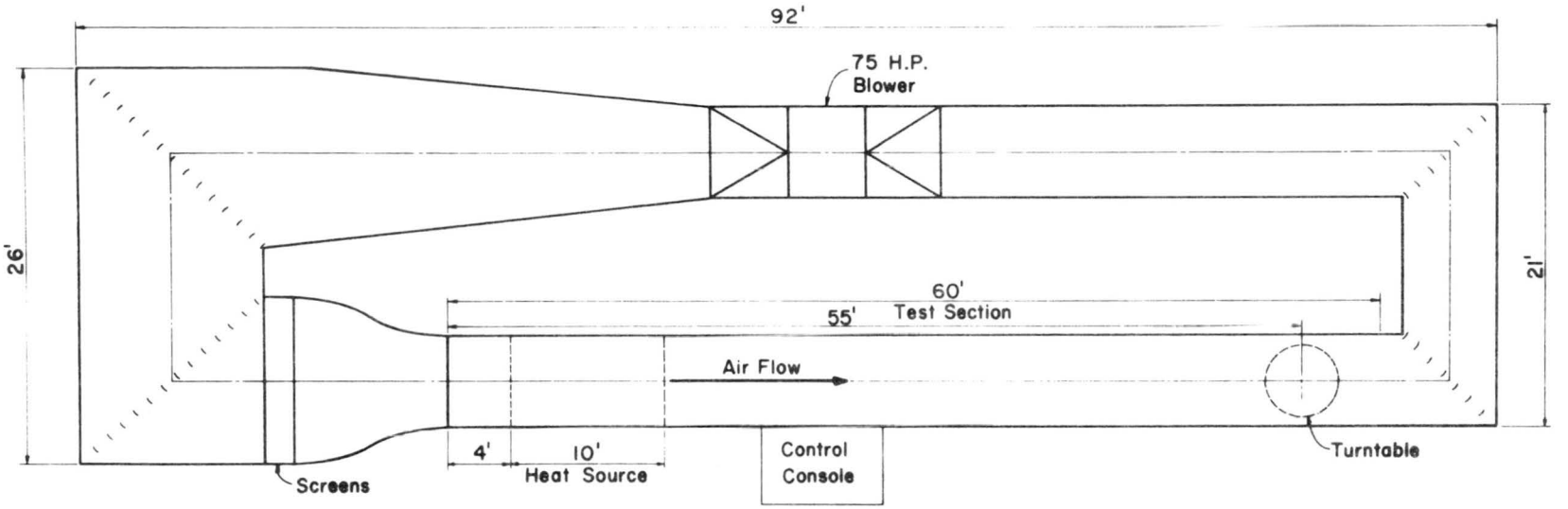

PLAN

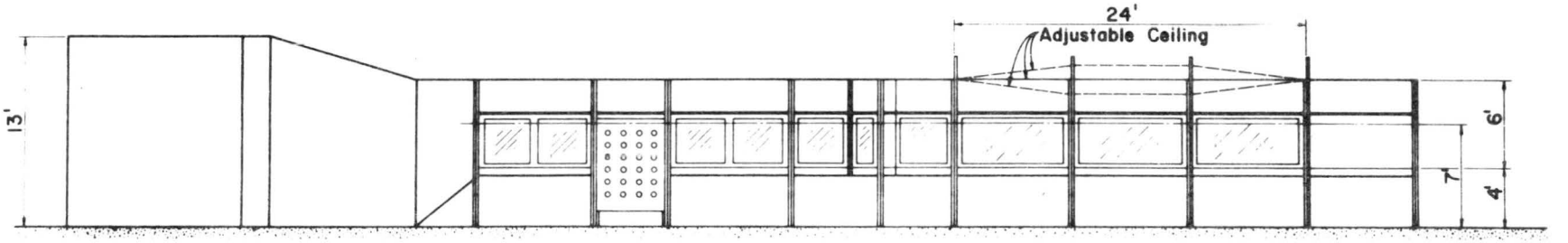

ELEVATION

Fig. 1. Industrial Aerodynamics Wind Tunnel
Fluid Dynamics & Diffusion Laboratory
Colorado State University

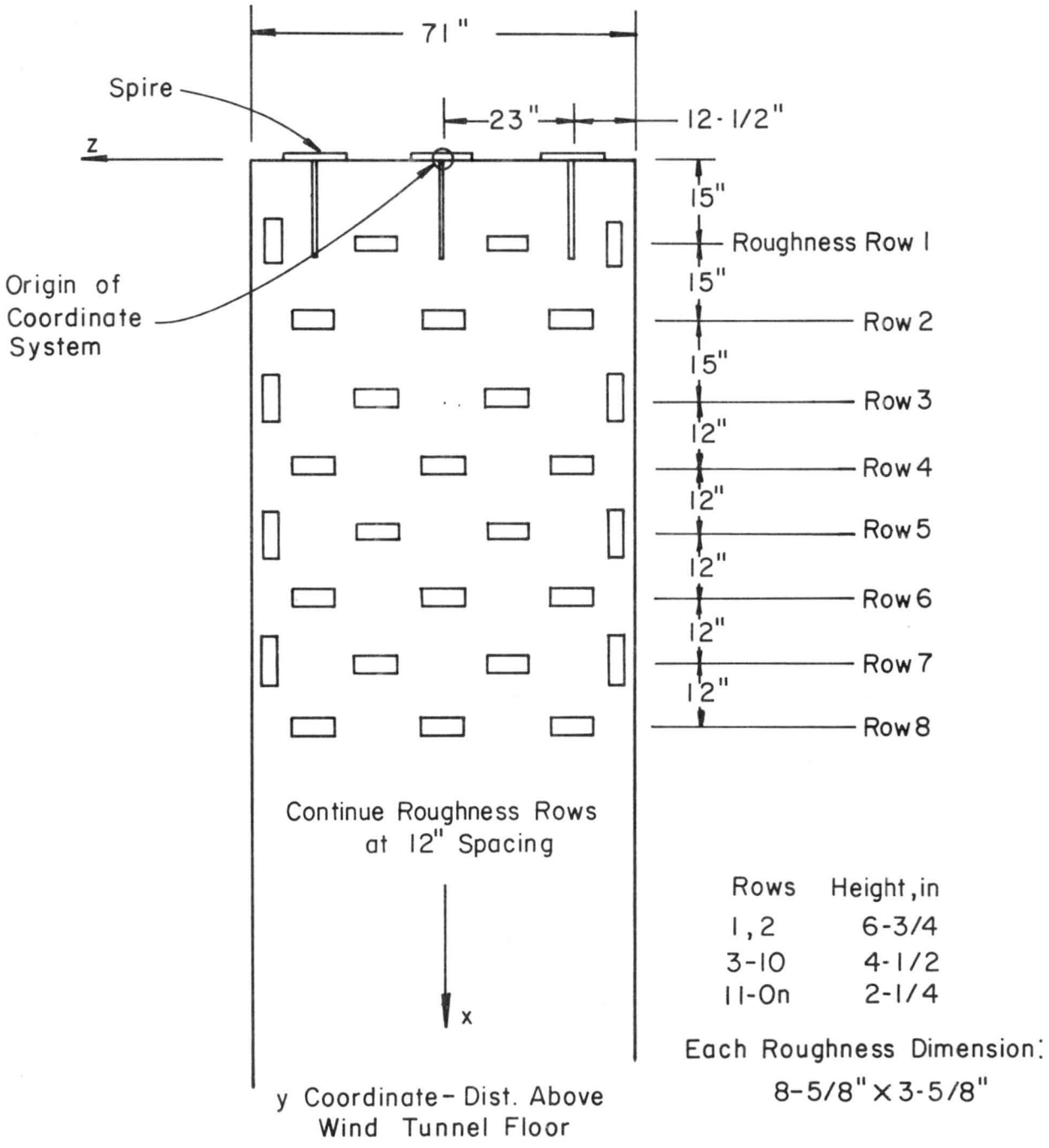

Wind Tunnel Configuration 1

Fig. 2. Spire and Roughness Arrays

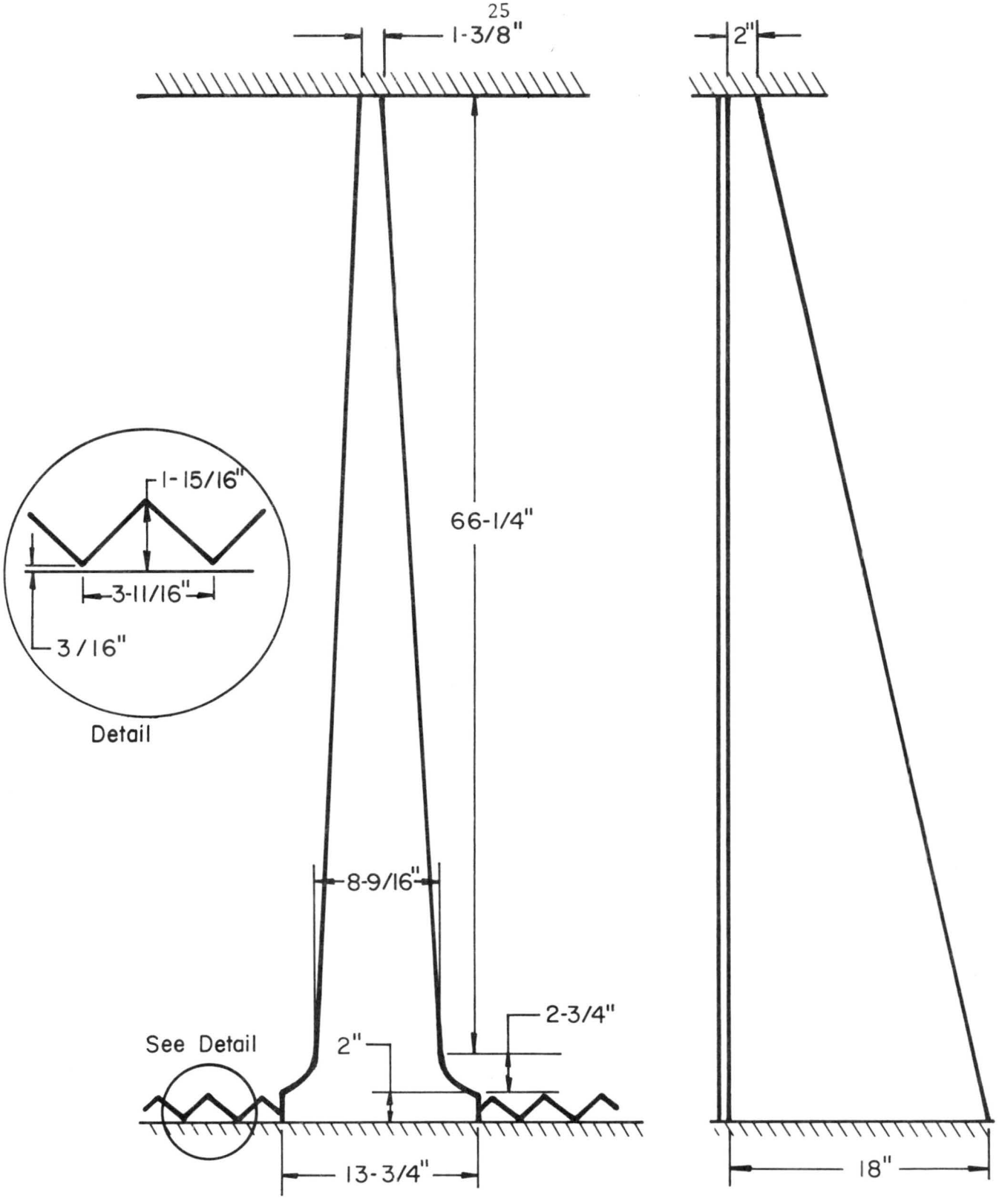

Fig. 2. Spire and Roughness Arrays (continued)

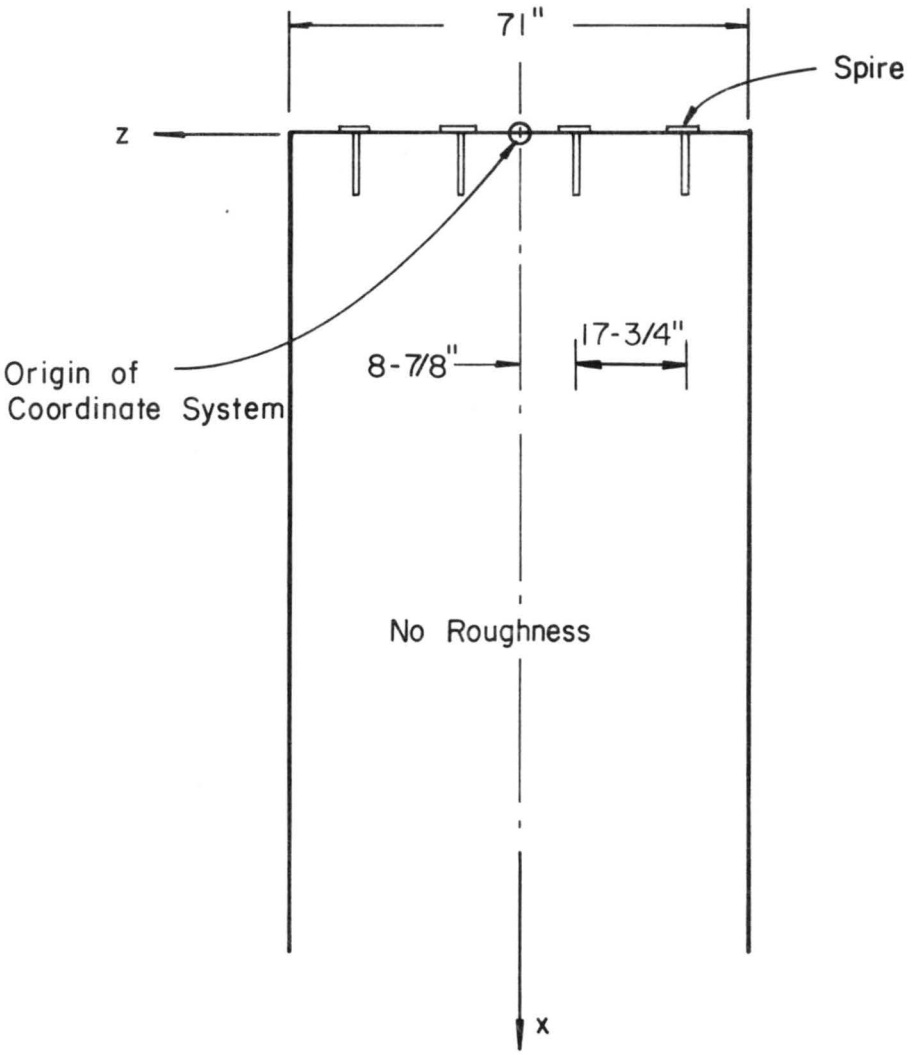

Fig. 2. Spire and Roughness Arrays (continued)

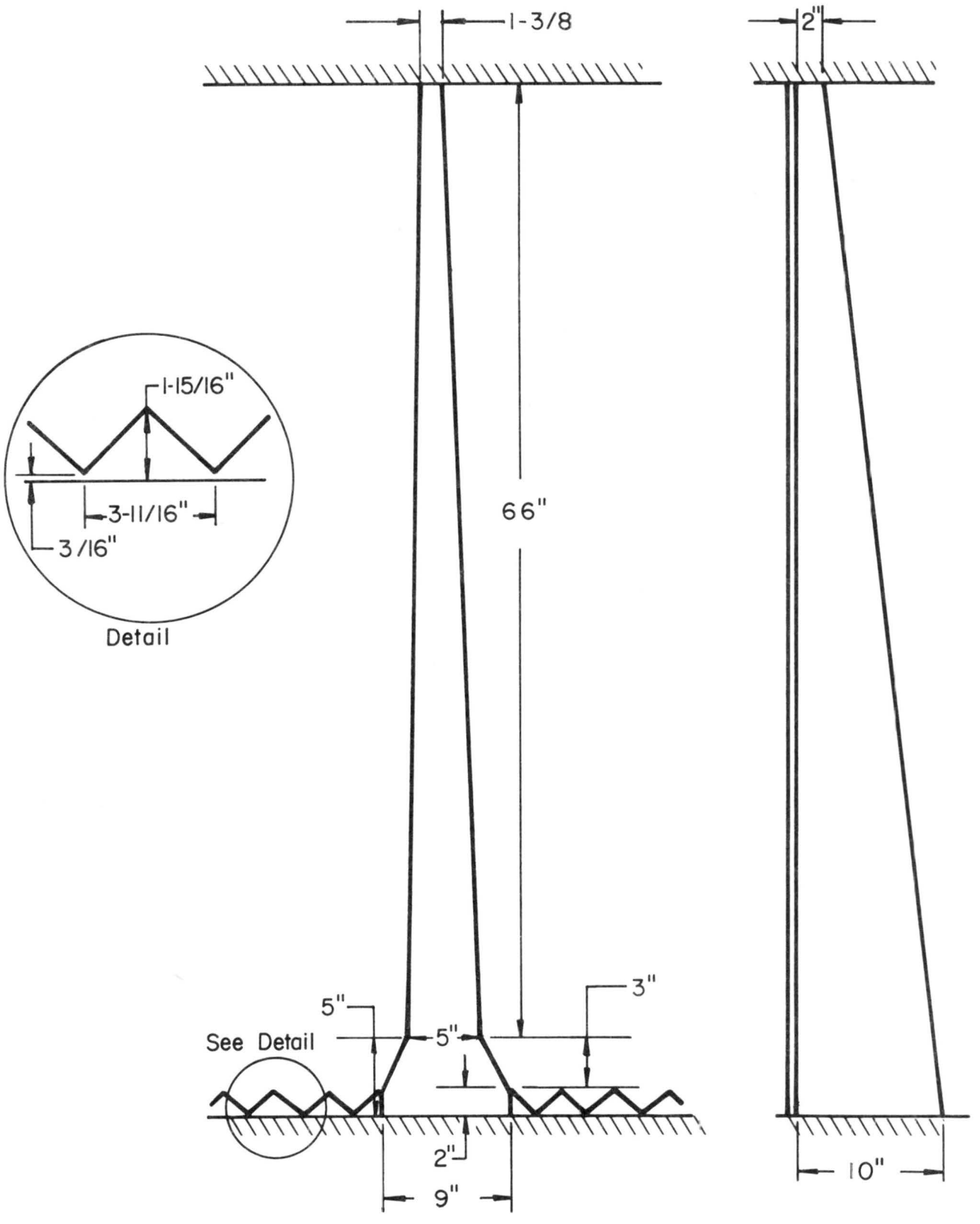

Spire for Configuration 2

Fig. 2. Spire and Roughness Arrays (continued)

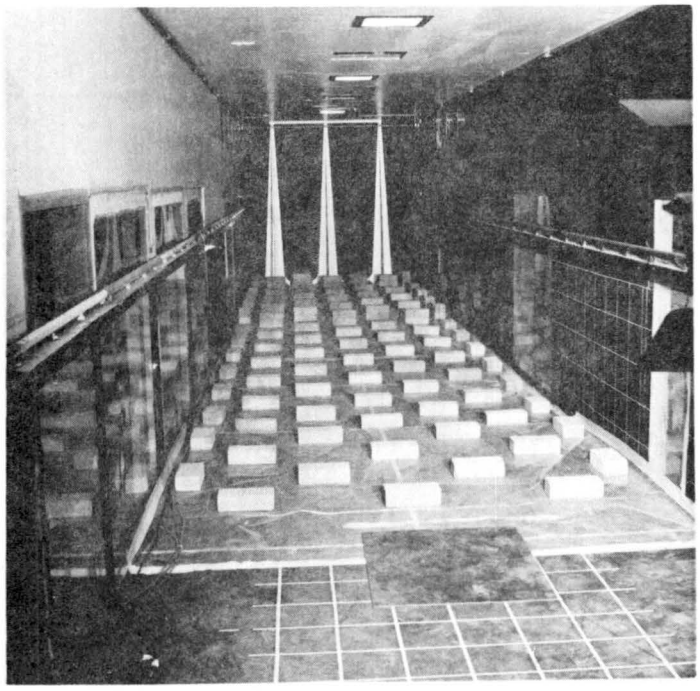

Configuration 1

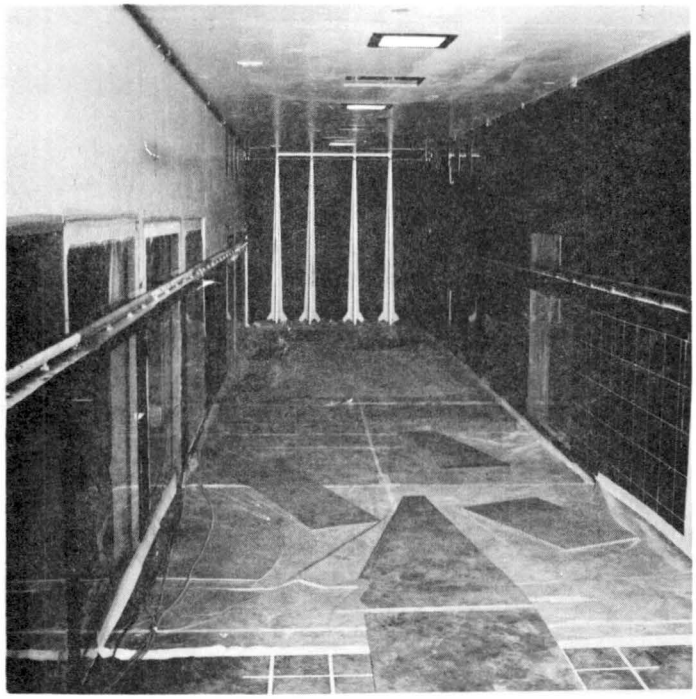

Configuration 2

Fig. 3. Spire and Roughness Arrays

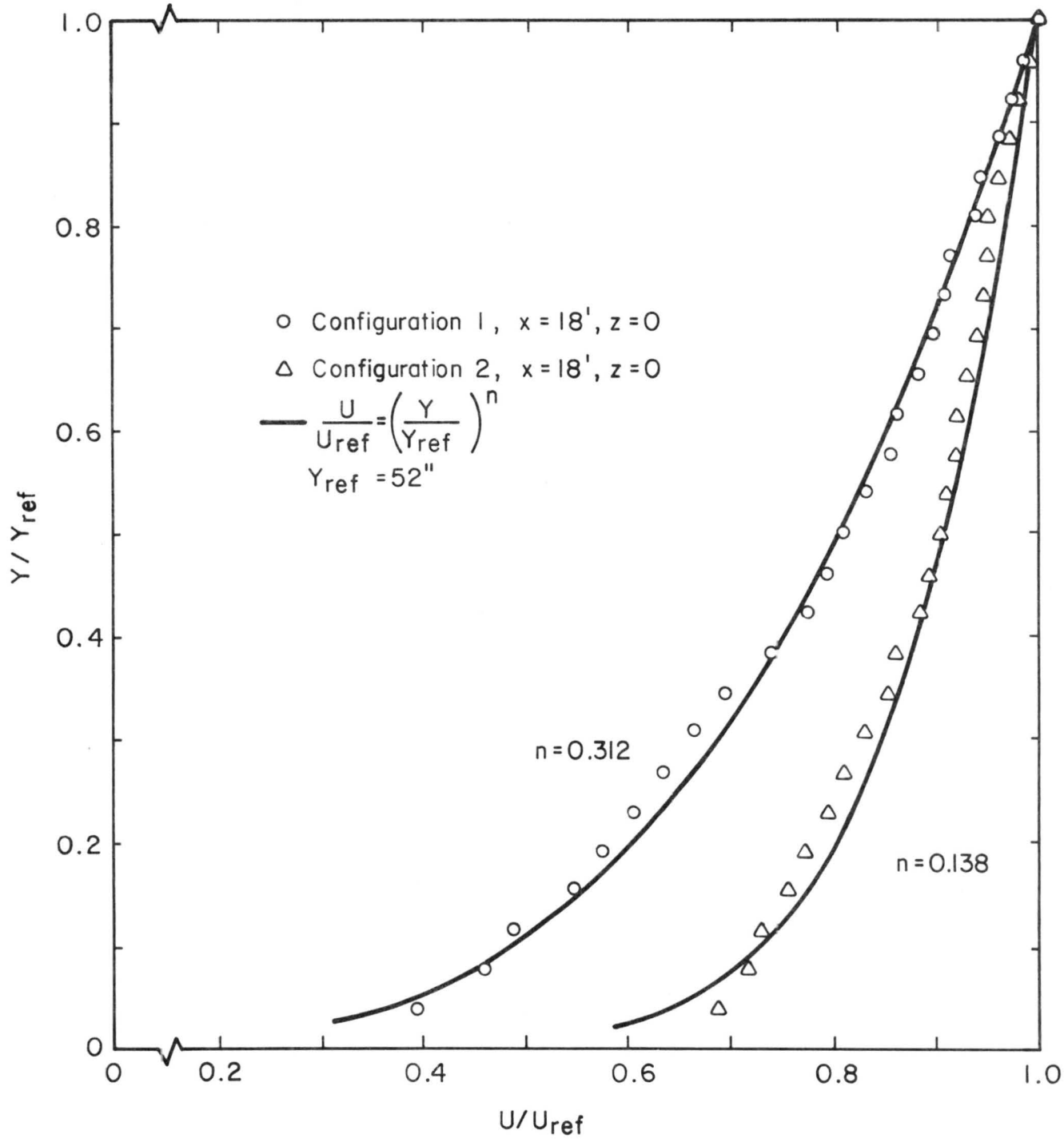

Fig. 4. Mean Velocity Profiles--Rectilinear Form

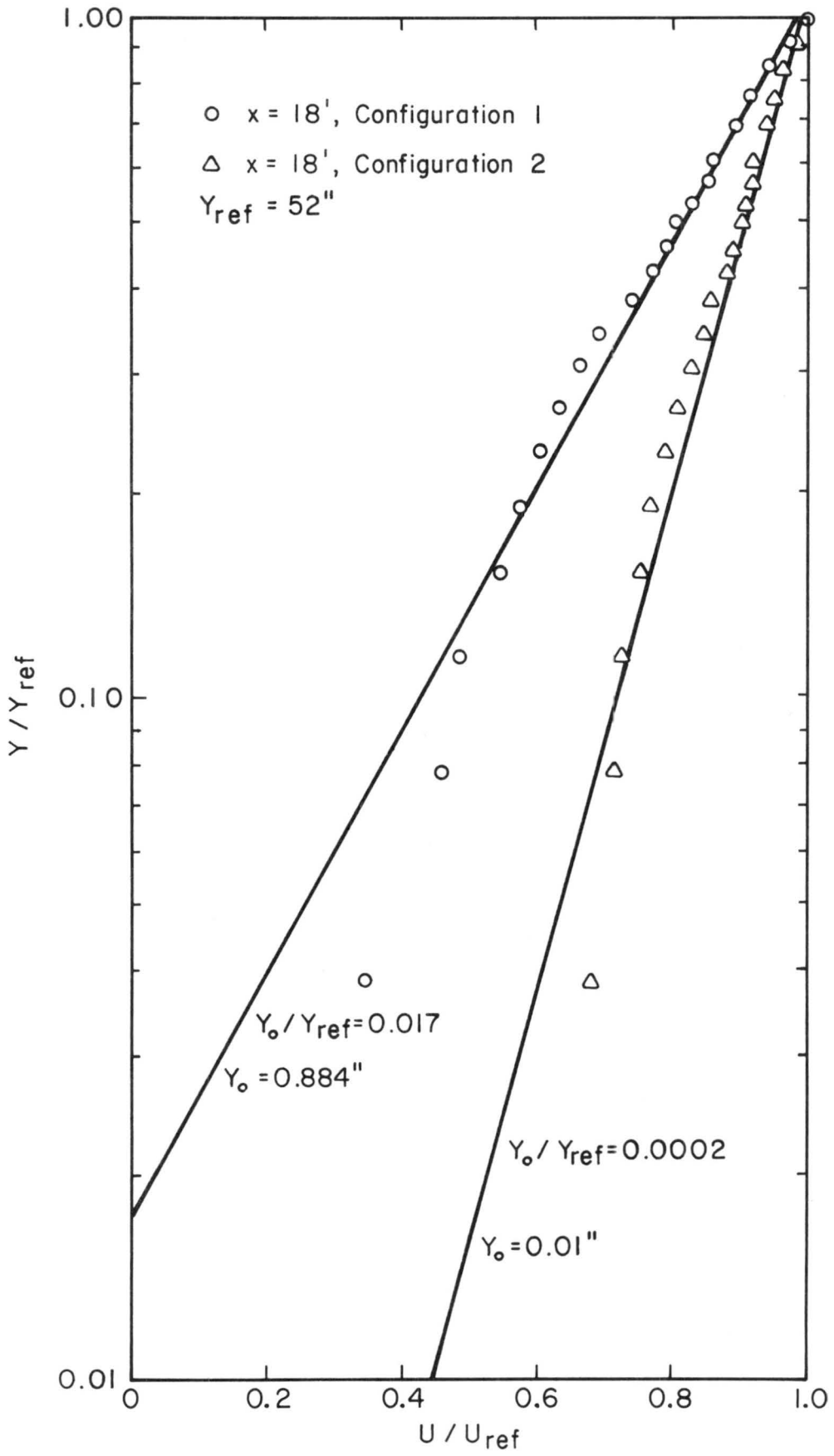

Fig. 5. Mean Velocity Profiles--Logarithmic Form

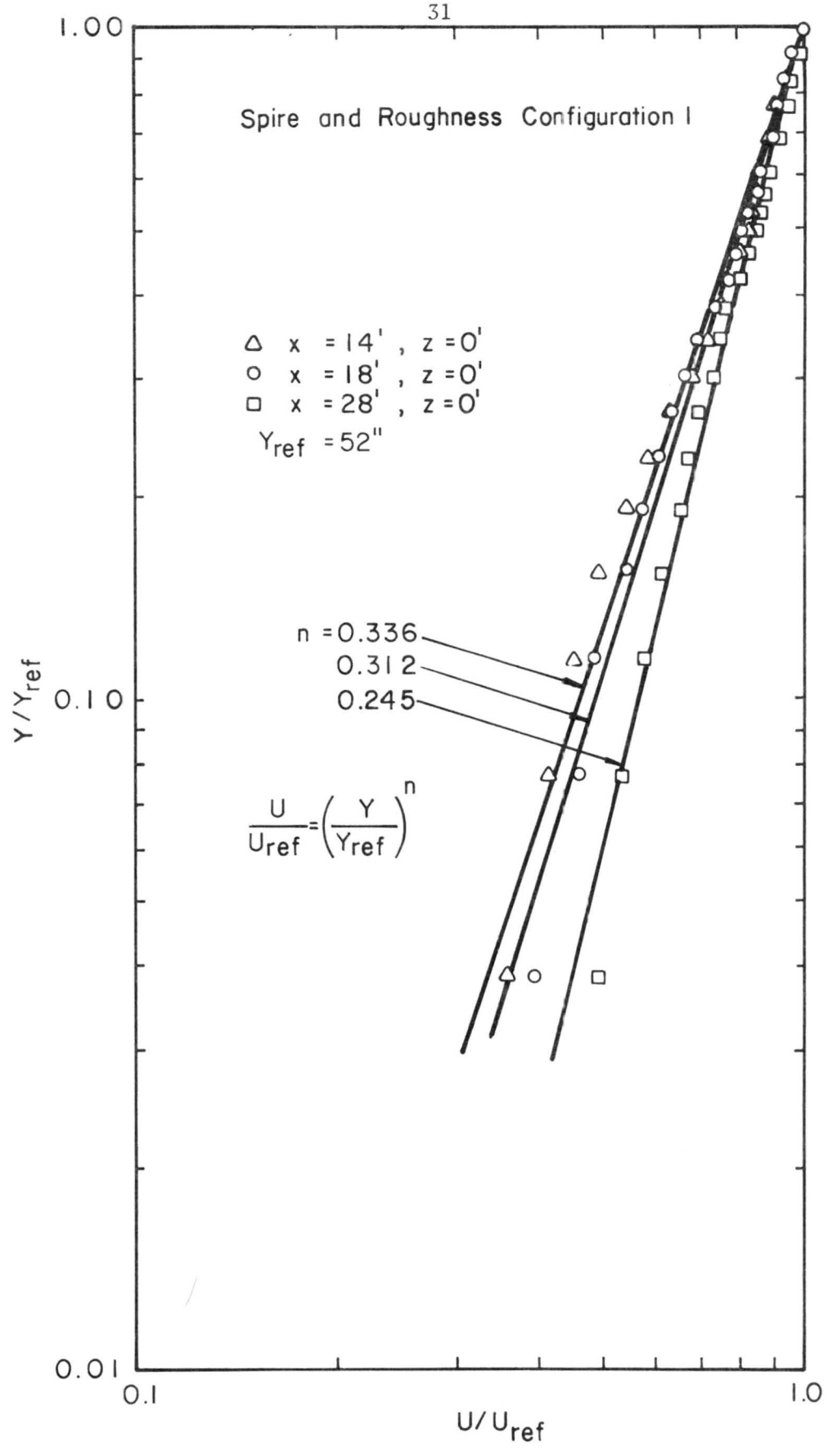

Fig. 6. Mean Velocity Profiles--Power Law Form--Variation with Longitudinal Position

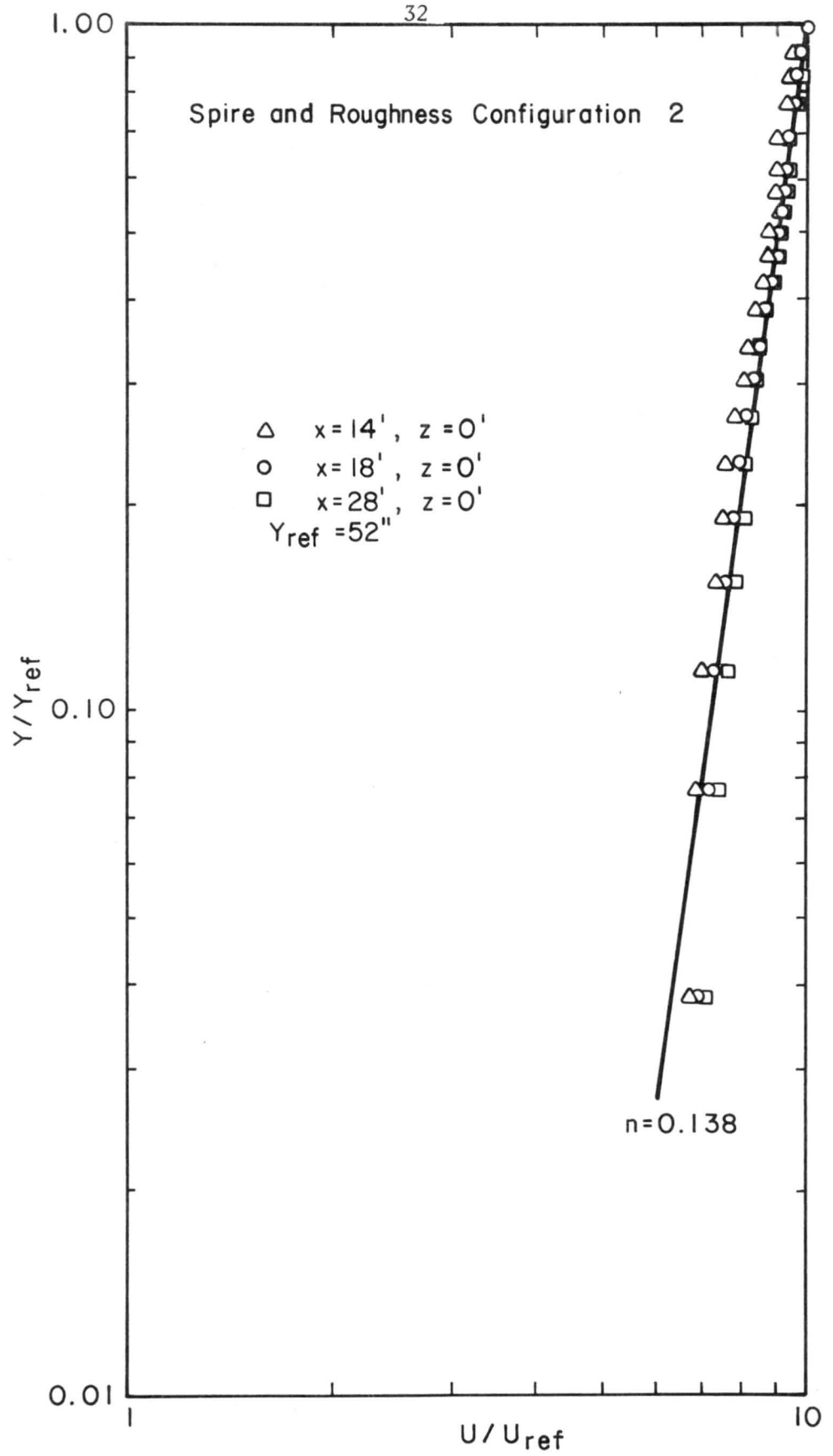

Fig. 6. Mean Velocity Profiles--Power Law Form--Variation with Longitudinal Position (continued)

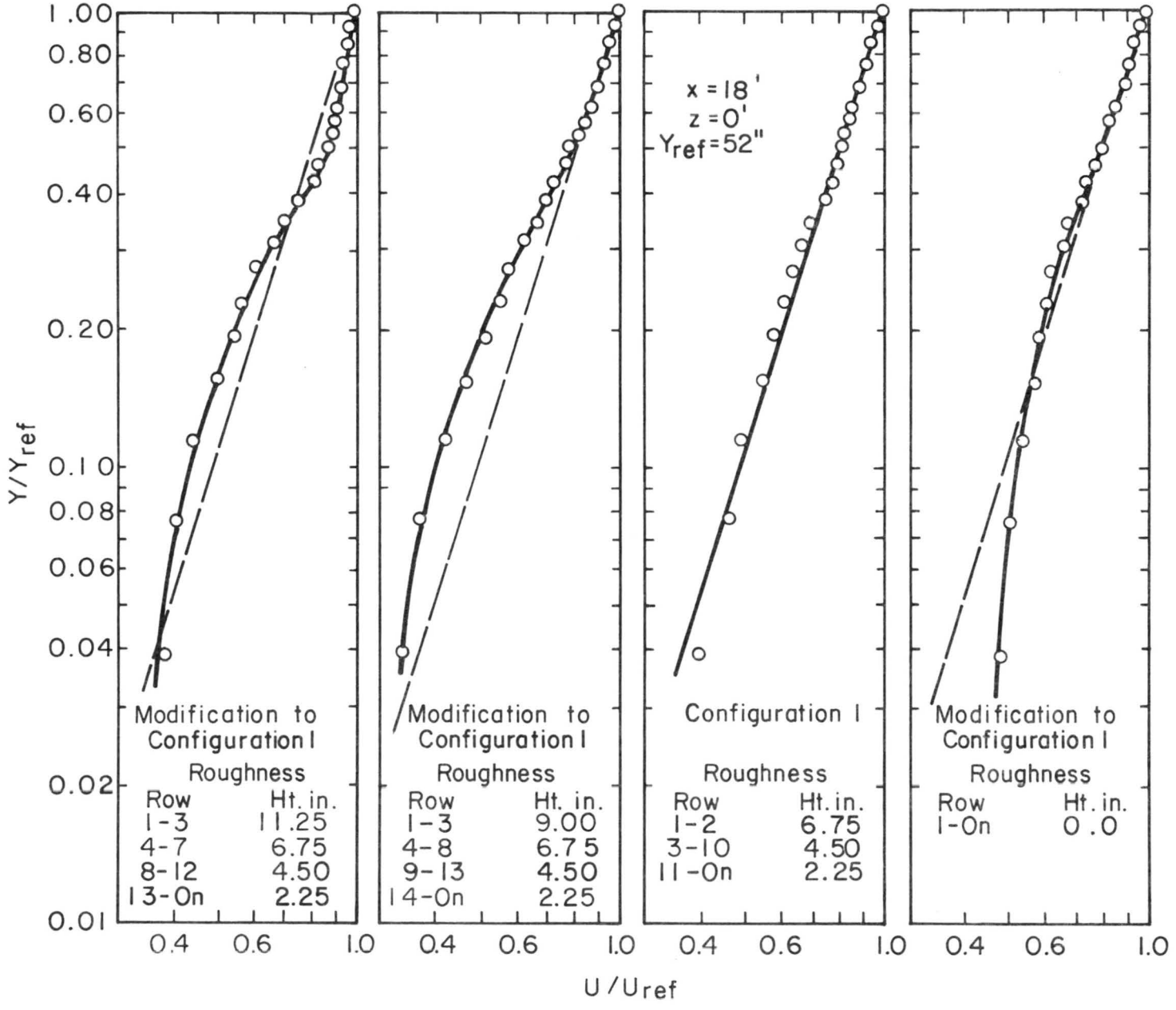

Fig. 7. Mean Velocity Profiles--Variation with Roughness Height

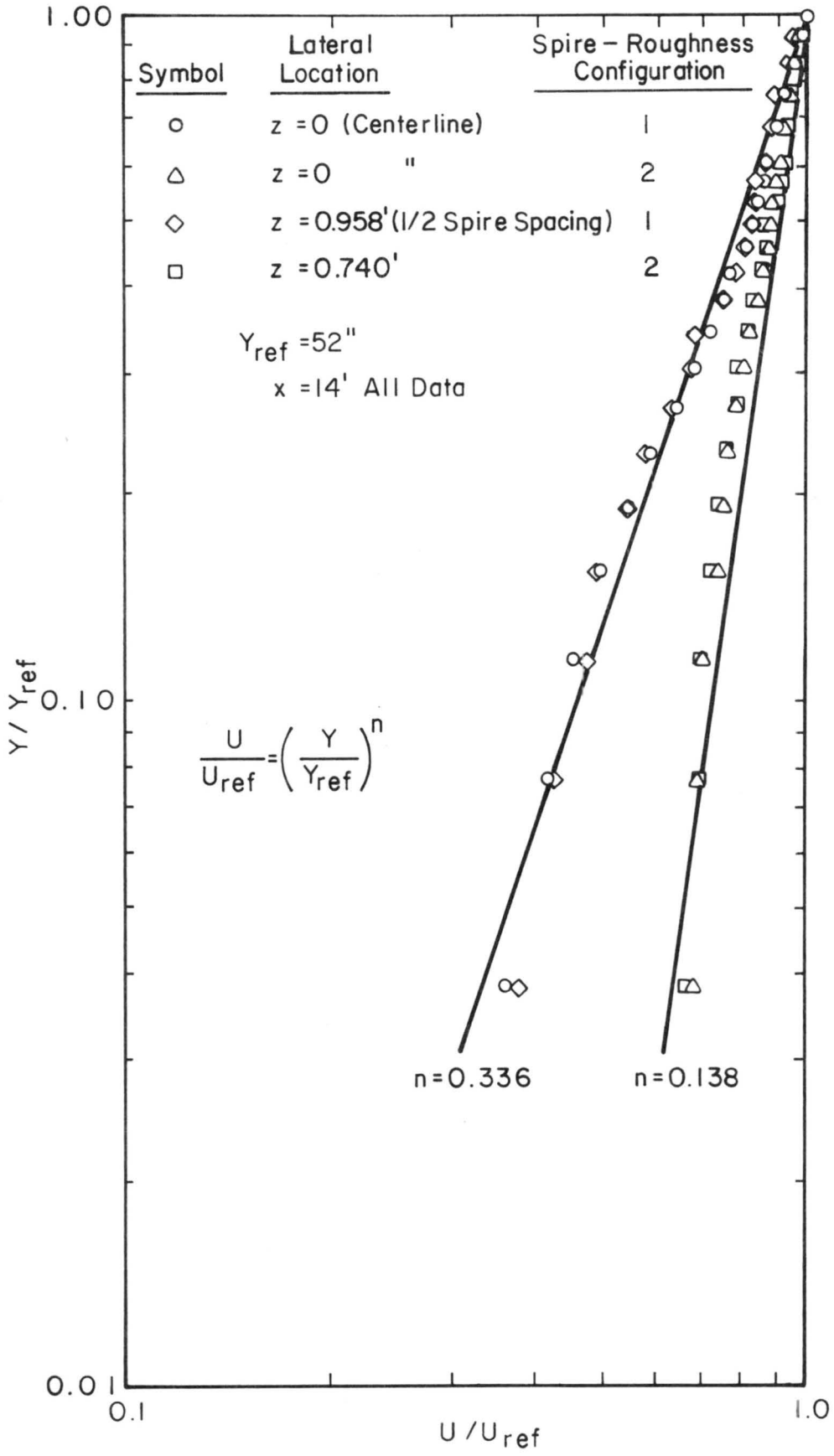

Fig. 8. Mean Velocity Profiles--Variation with Lateral Position

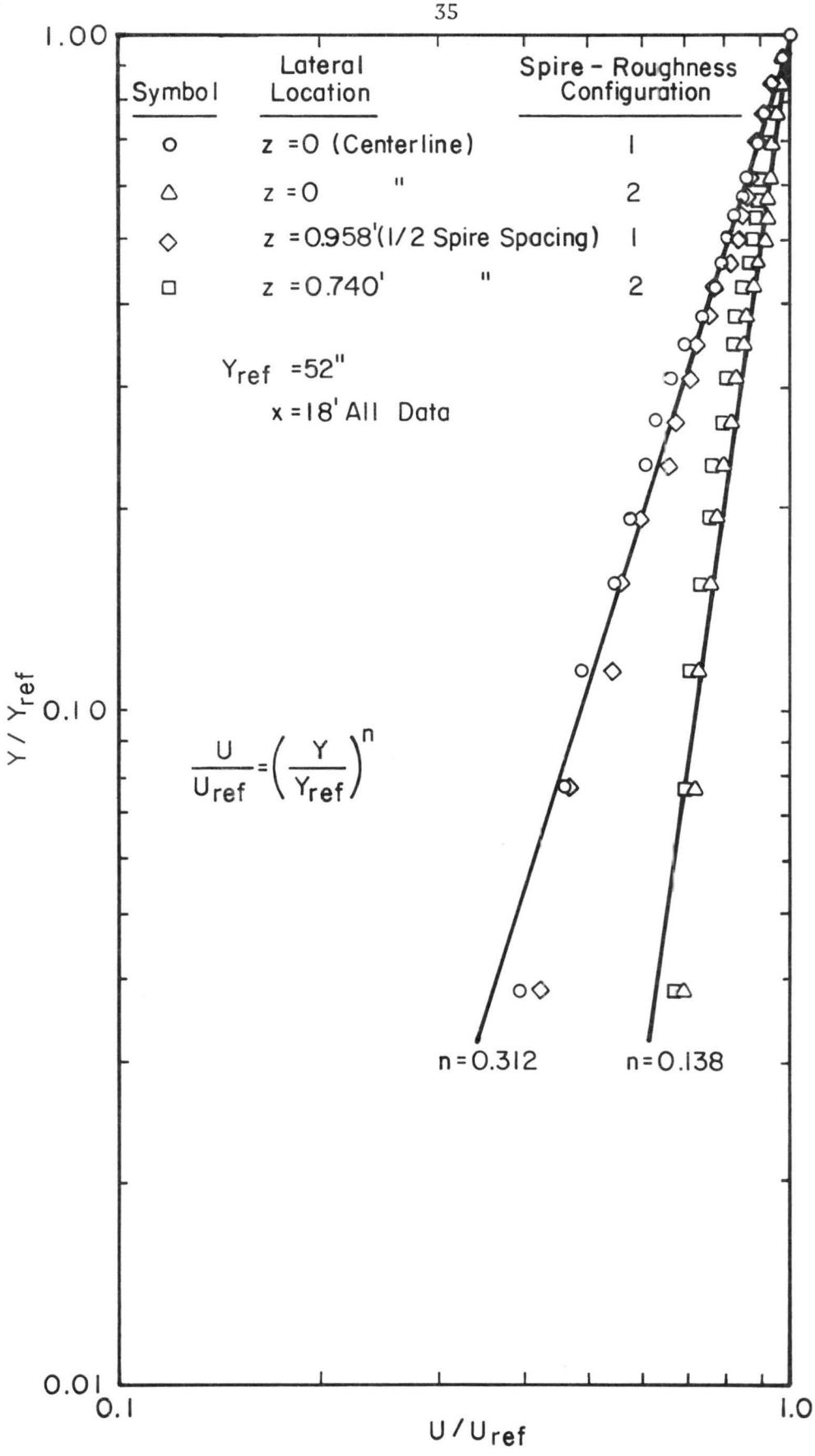

Fig. 8. Mean Velocity Profiles--Variation with Lateral Position (continued)

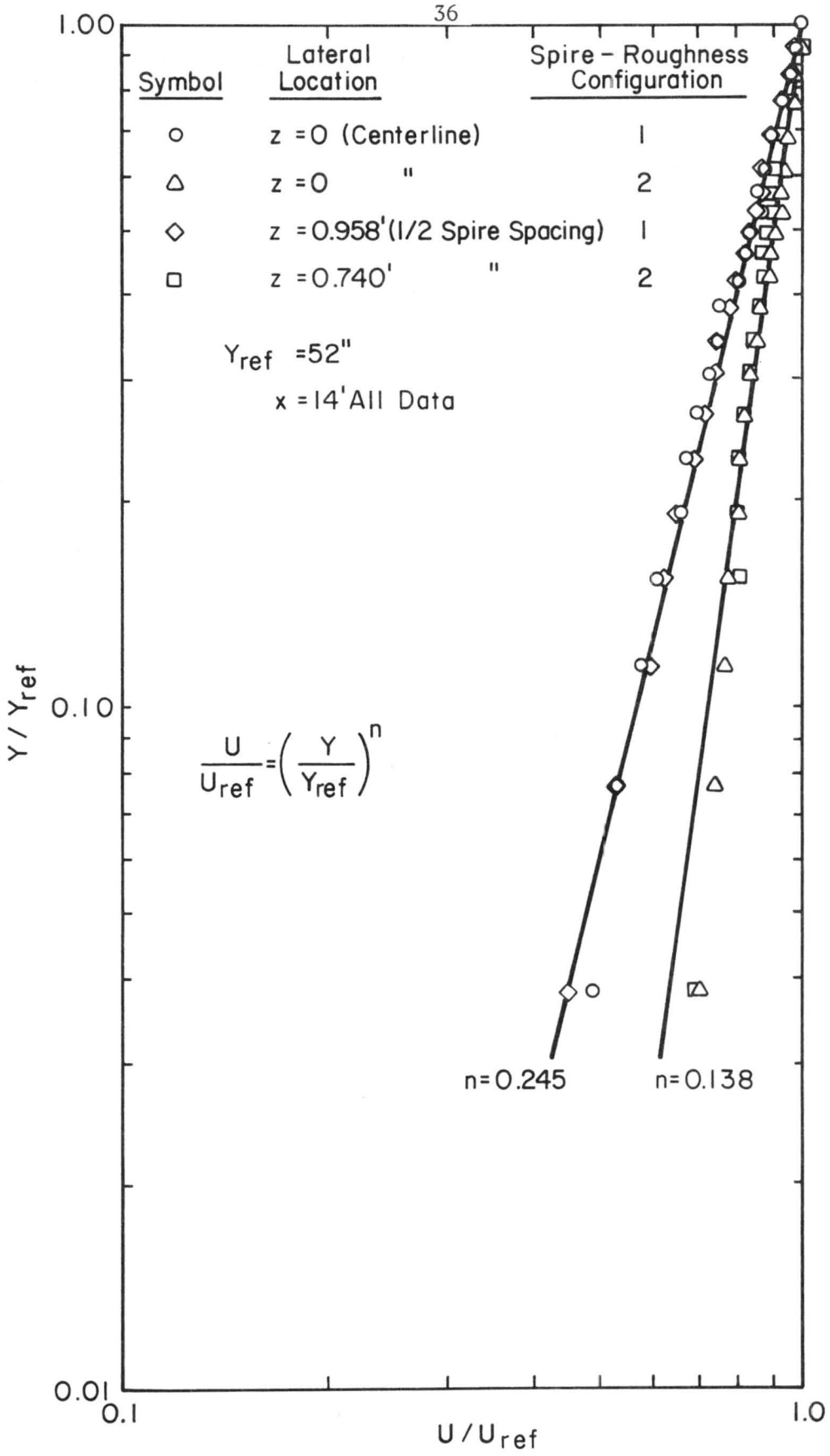

Fig. 8. Mean Velocity Profiles--Variation with Lateral Position (continued)

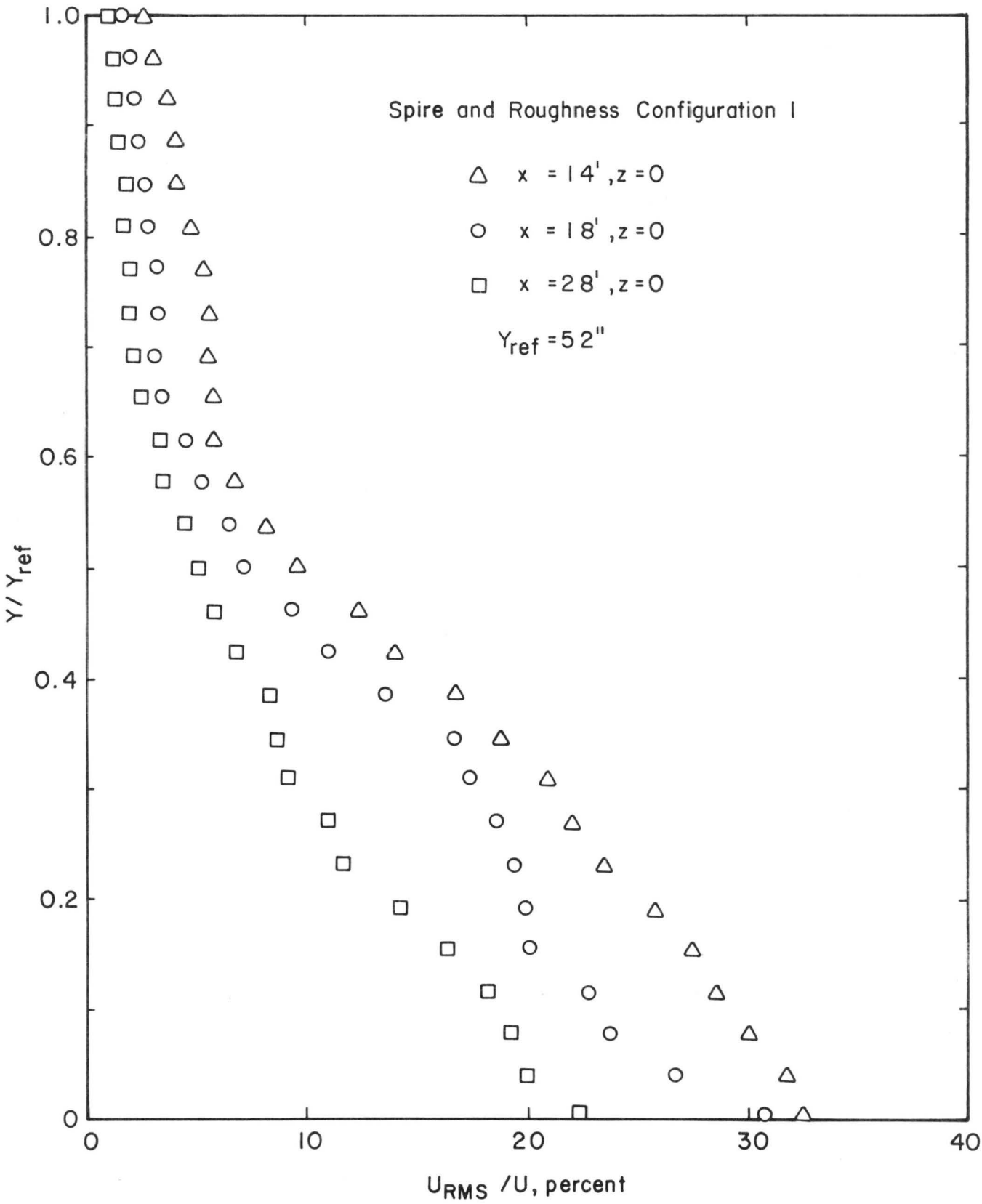

Fig. 9. Turbulence Intensity--Variation with Longitudinal Position--Configuration 1

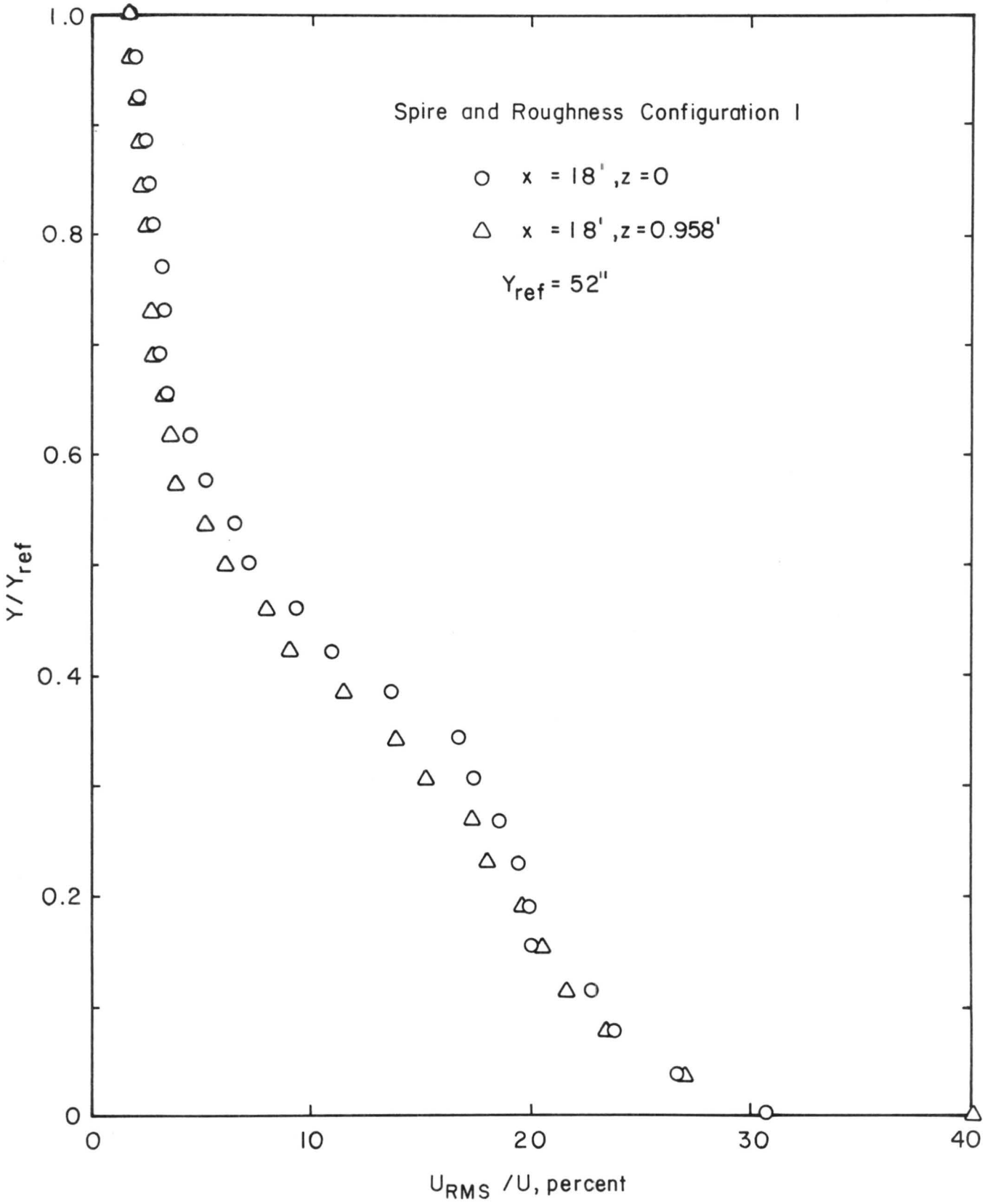

Fig. 10. Turbulence Intensity--Variation with Lateral Position--Configuration 1

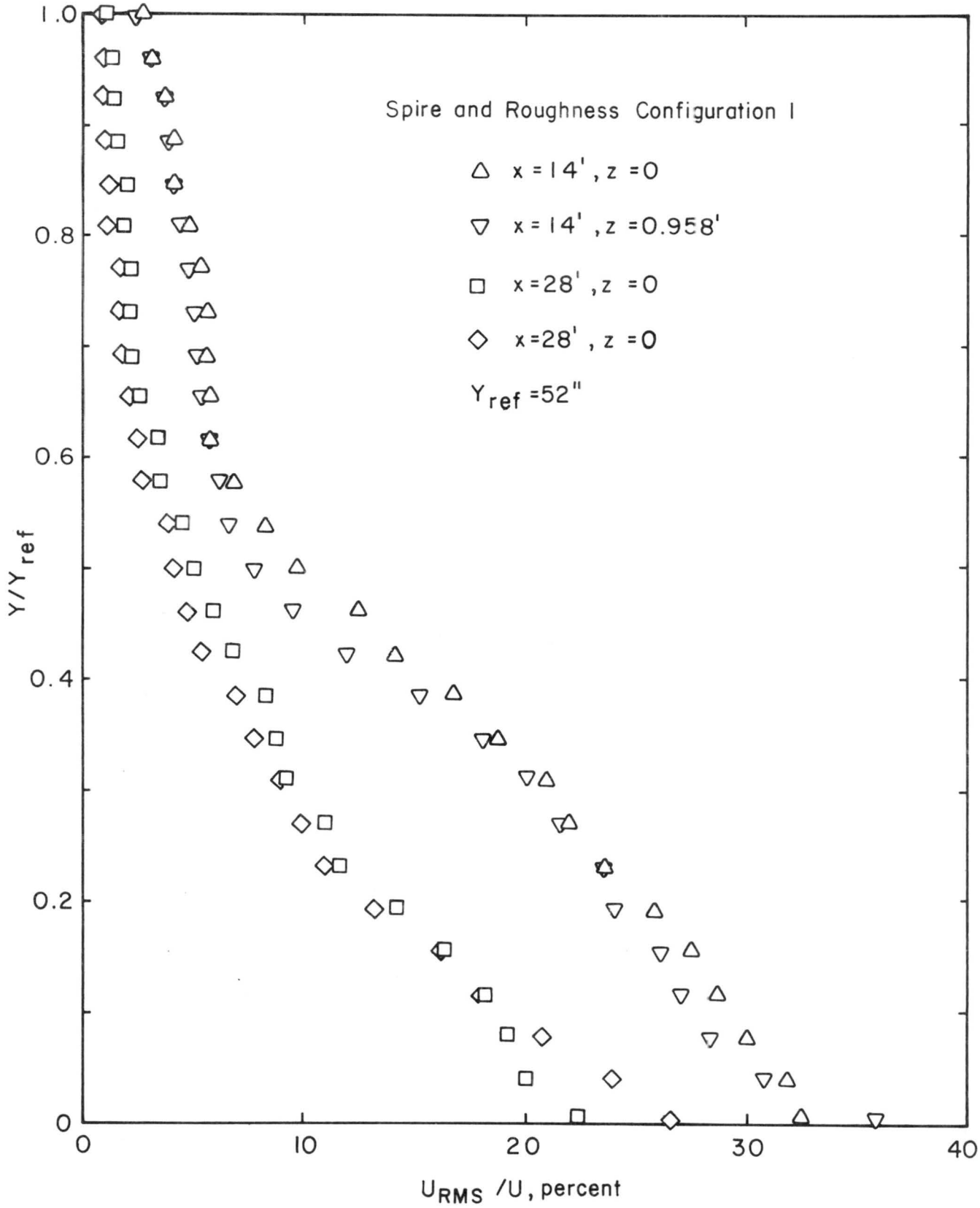

Fig. 10. Turbulence Intensity--Variation with Lateral Position--Configuration 1 (continued)

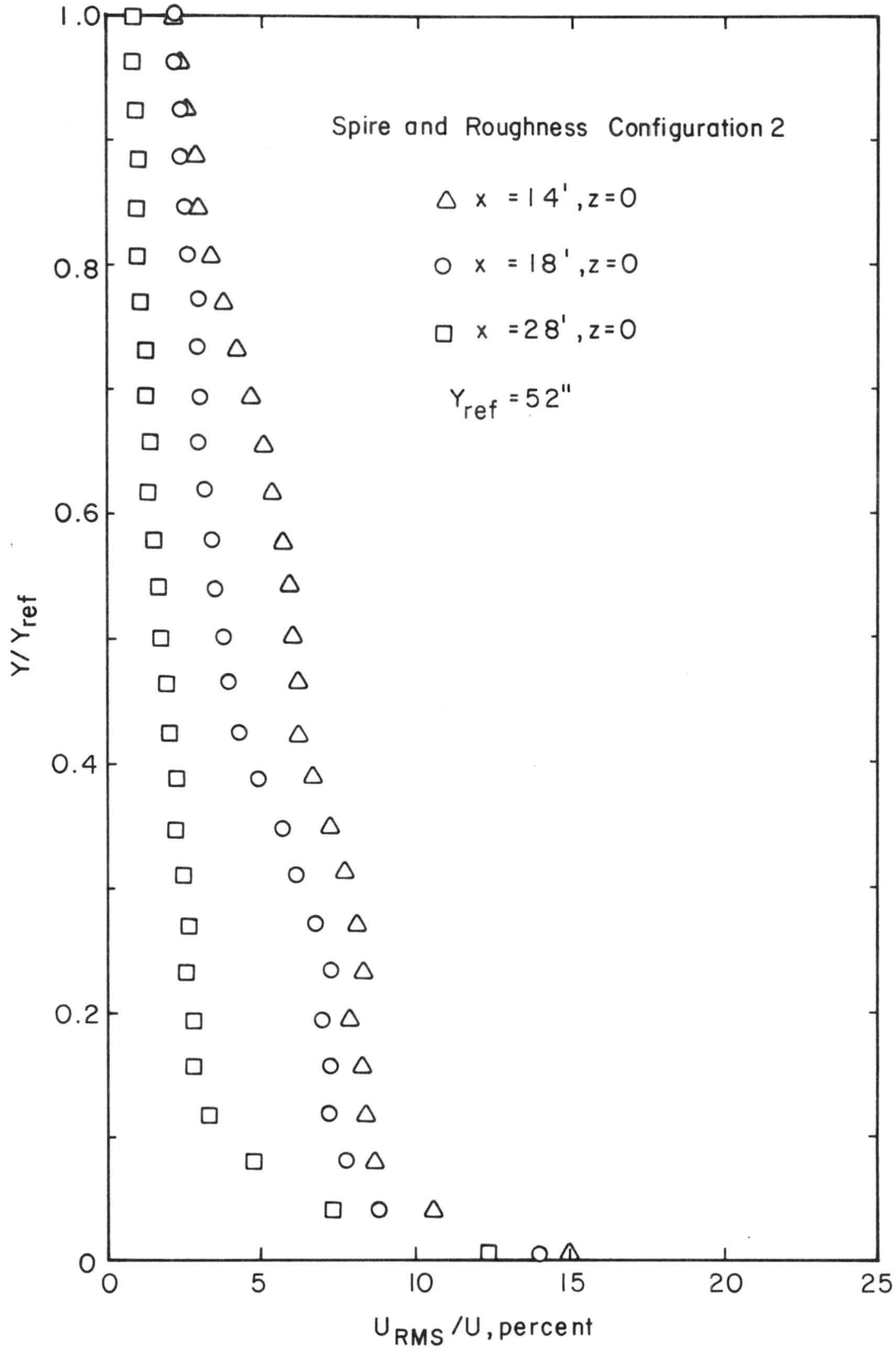

Fig. 11. Turbulence Intensity--Variation with Longitudinal Position--Configuration 2

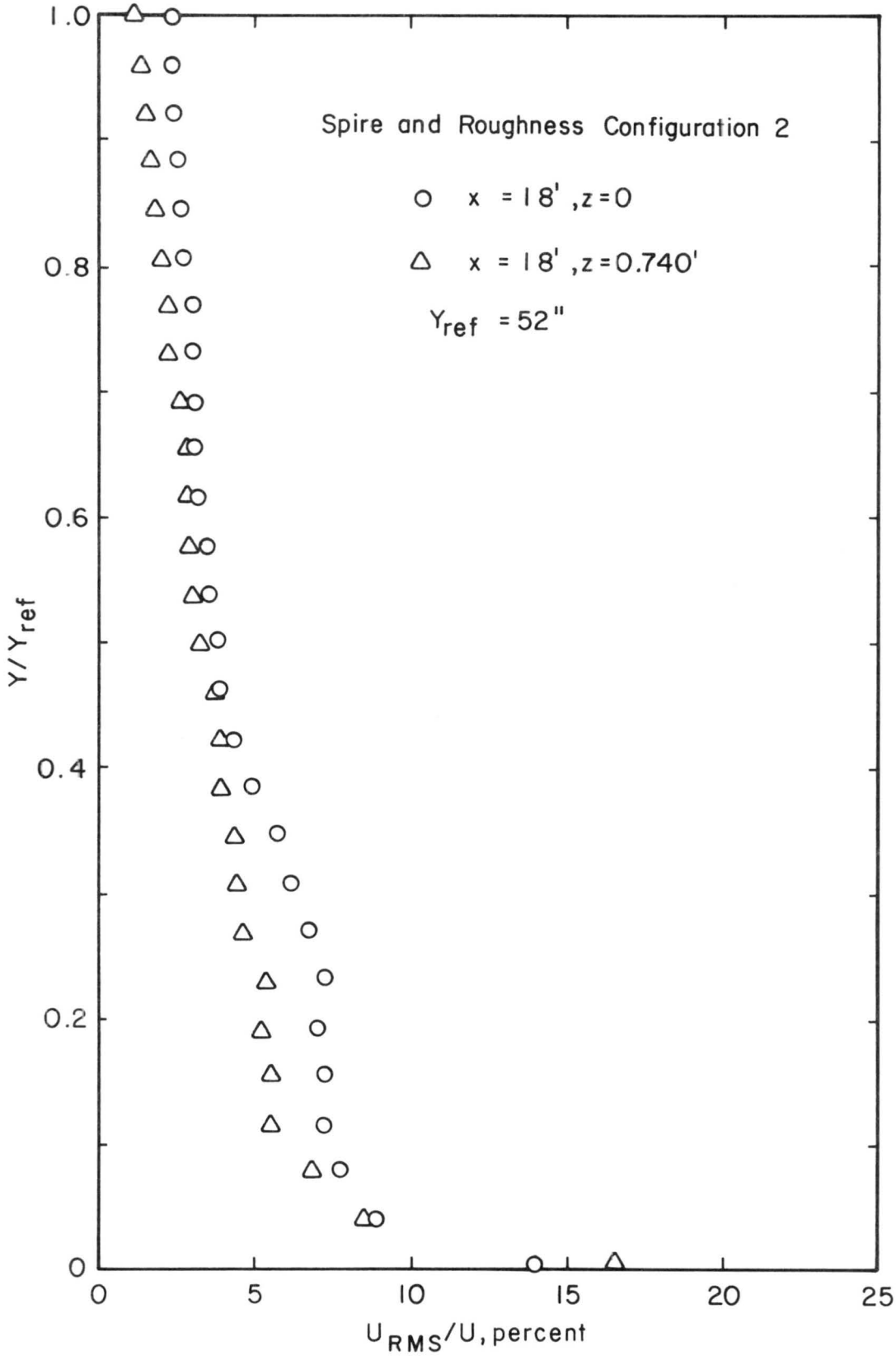

Fig. 12. Turbulence Intensity--Variation with Lateral Position--Configuration 2

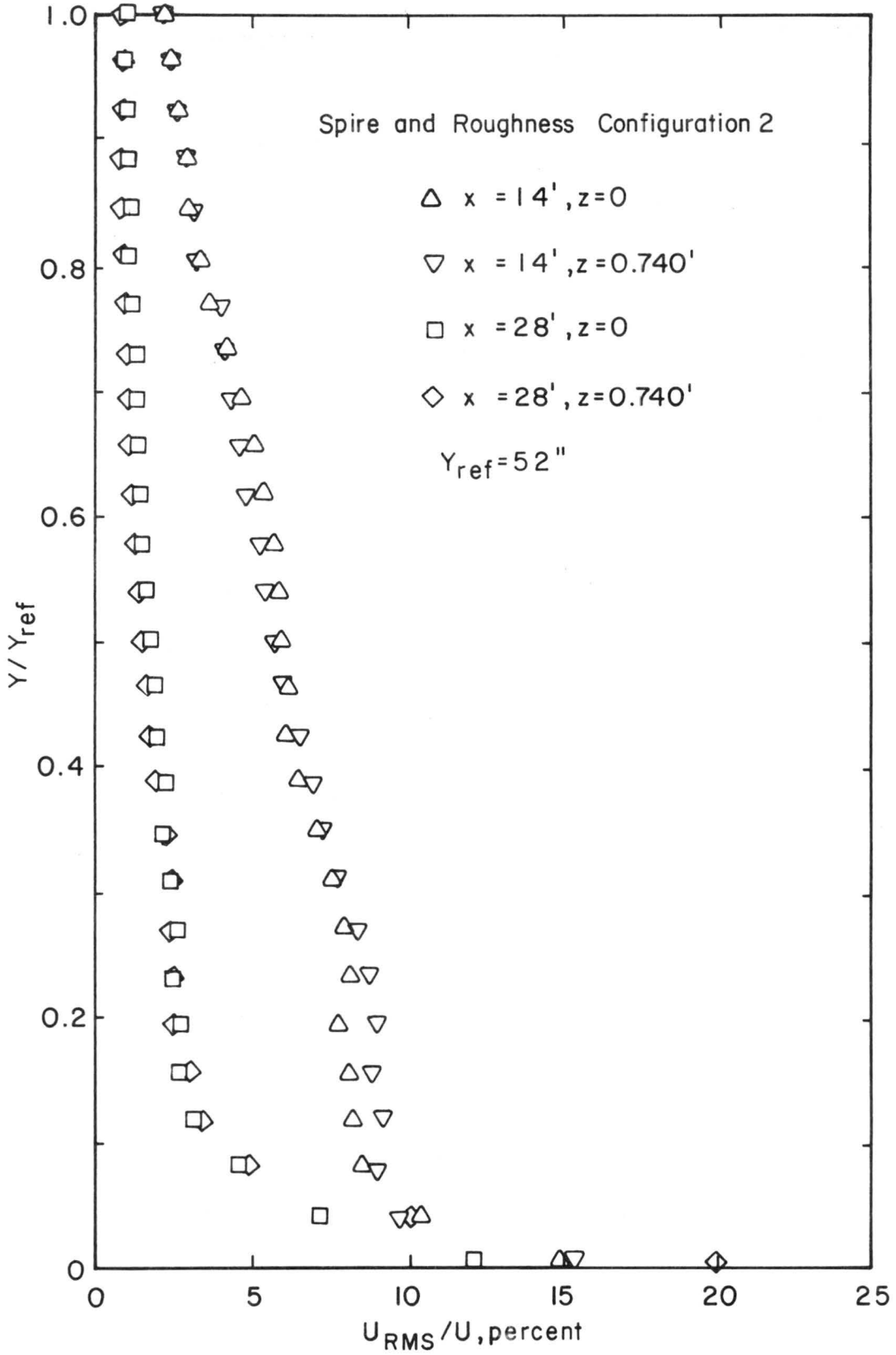

Fig. 12. Turbulence Intensity--Variation with Lateral Position--Configuration 2 (continued)

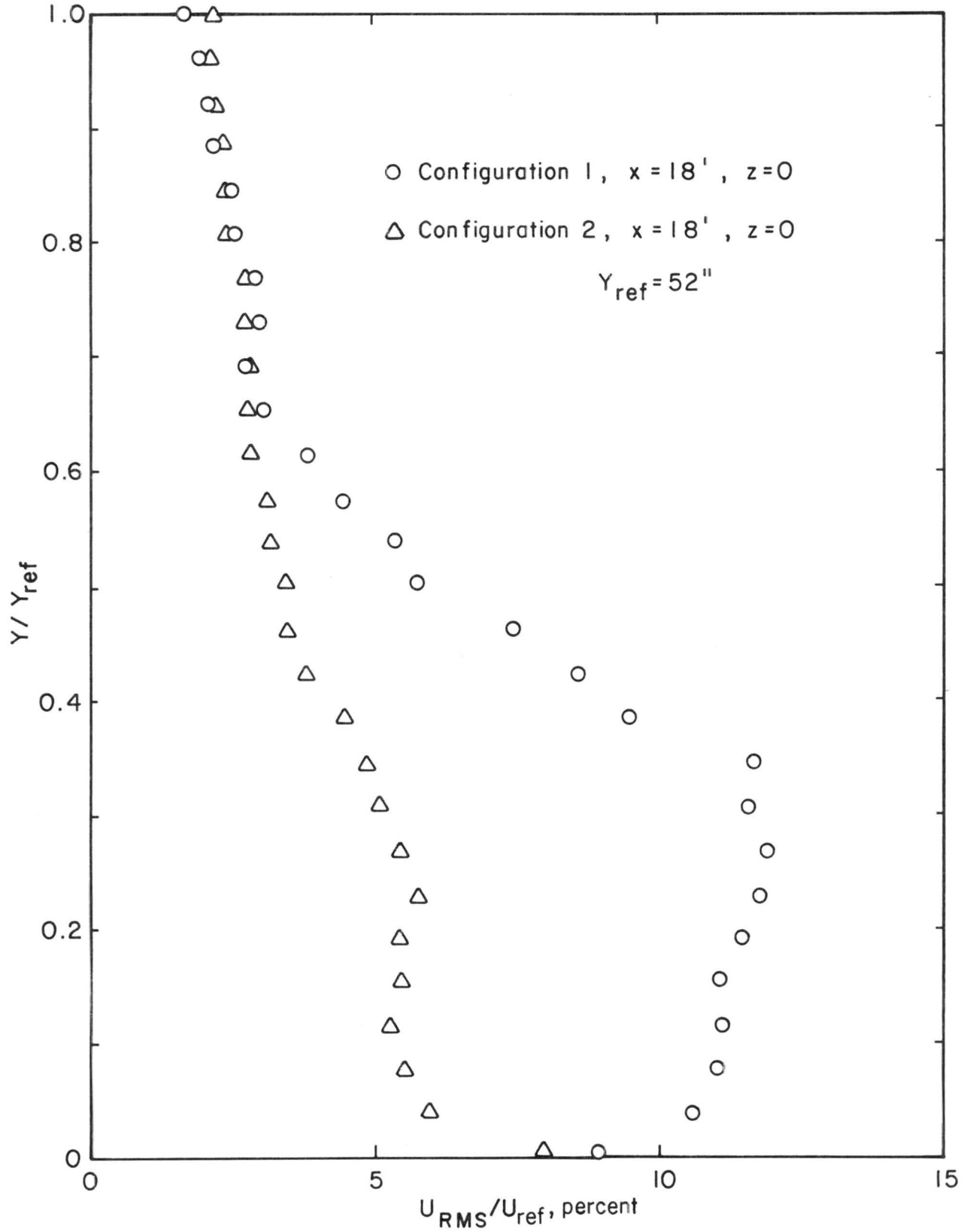

Fig. 13. Turbulence Intensity--Referenced to U_{ref}

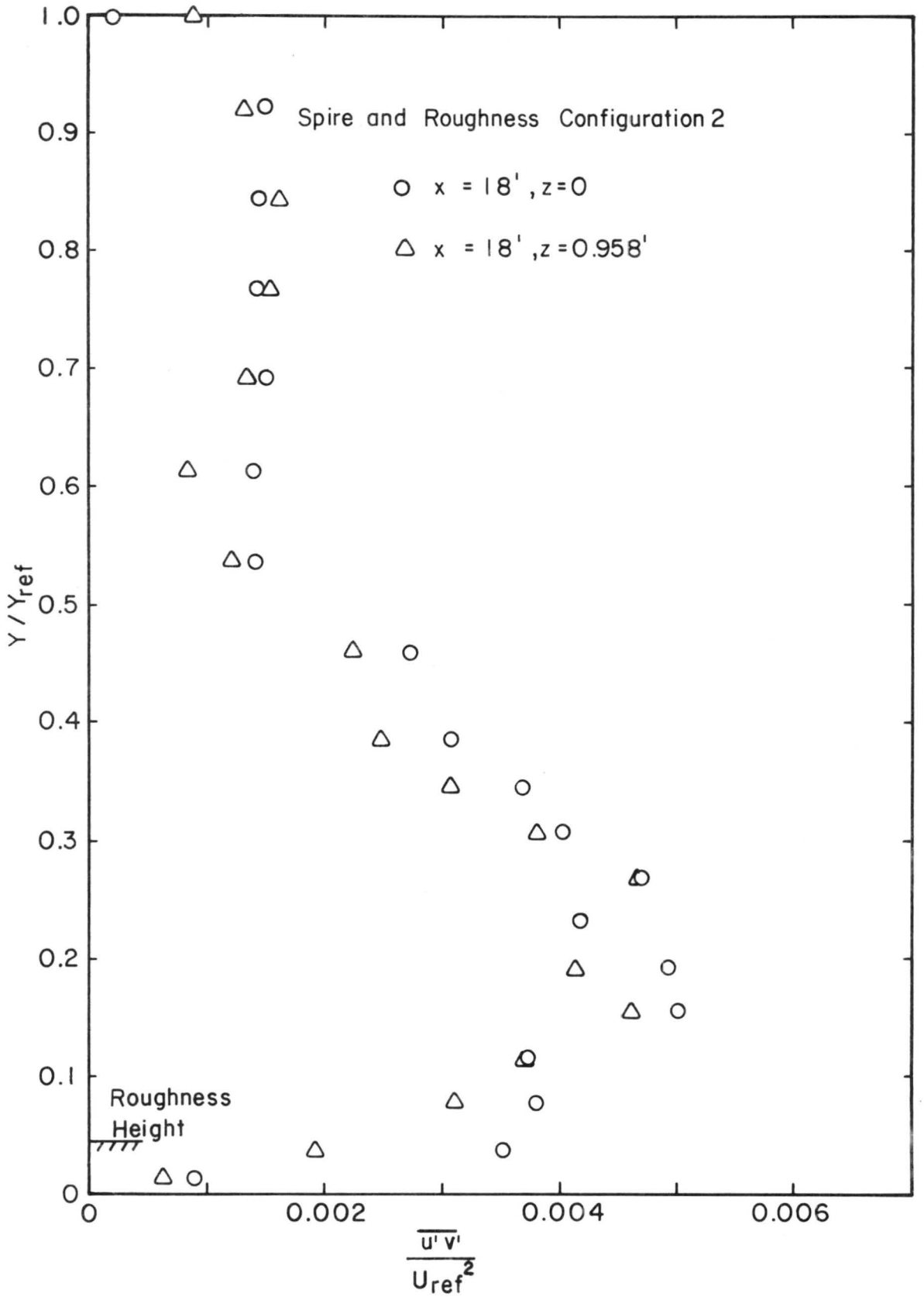

Fig. 14. Shear Stress--Configuration 1

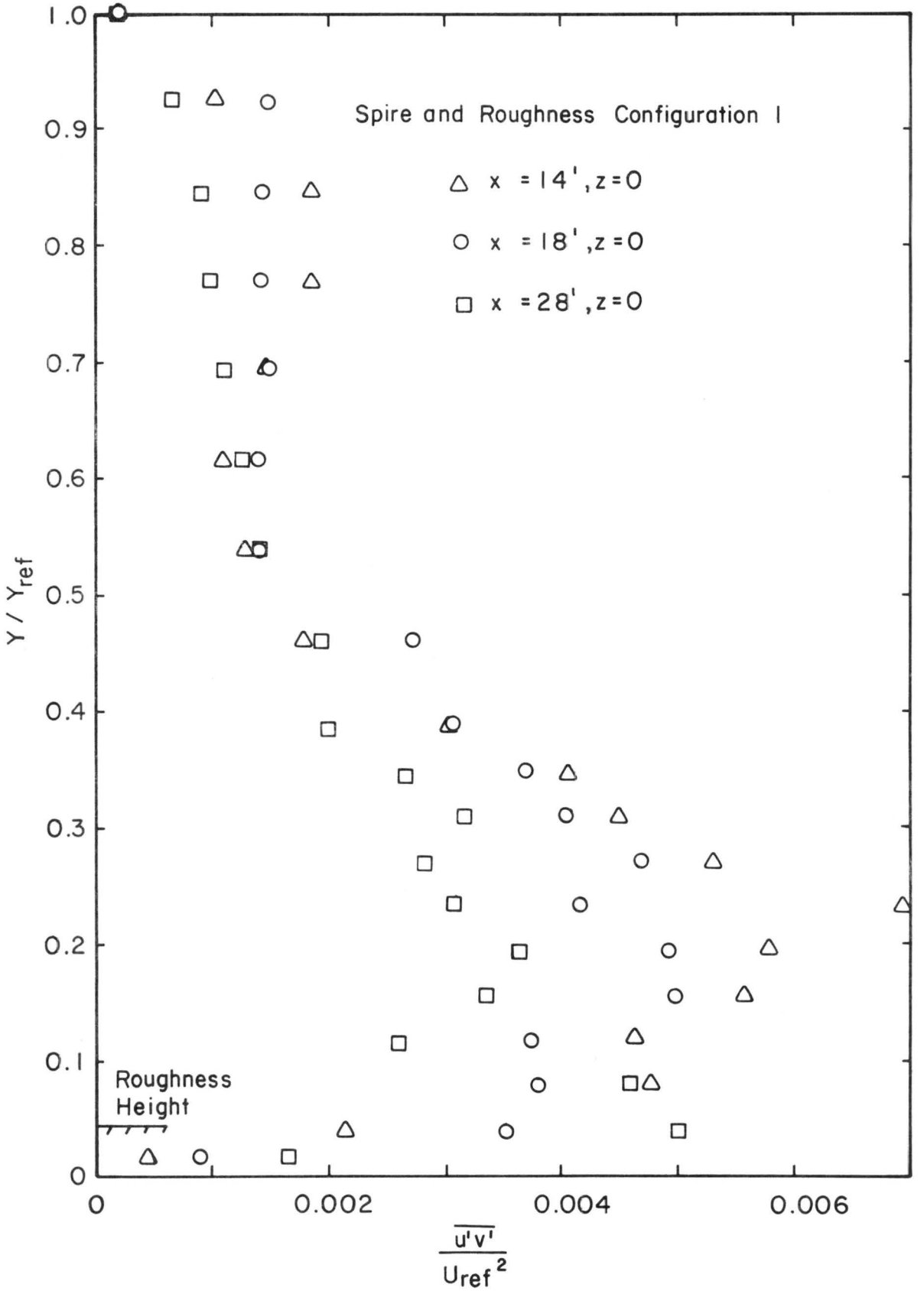

Fig. 14. Shear Stress--Configuration 1 (continued)

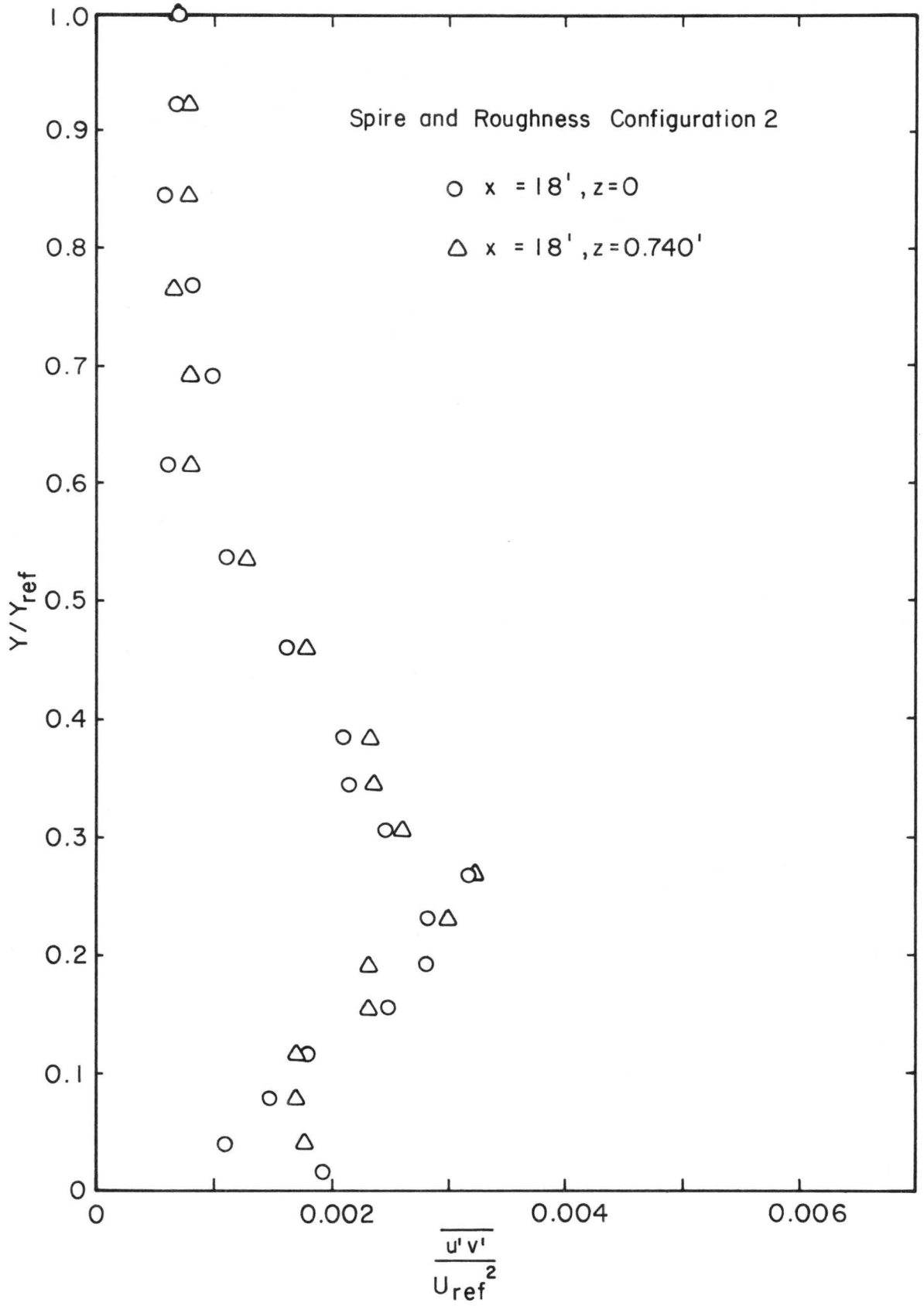

Fig. 15. Shear Stress--Configuration 2

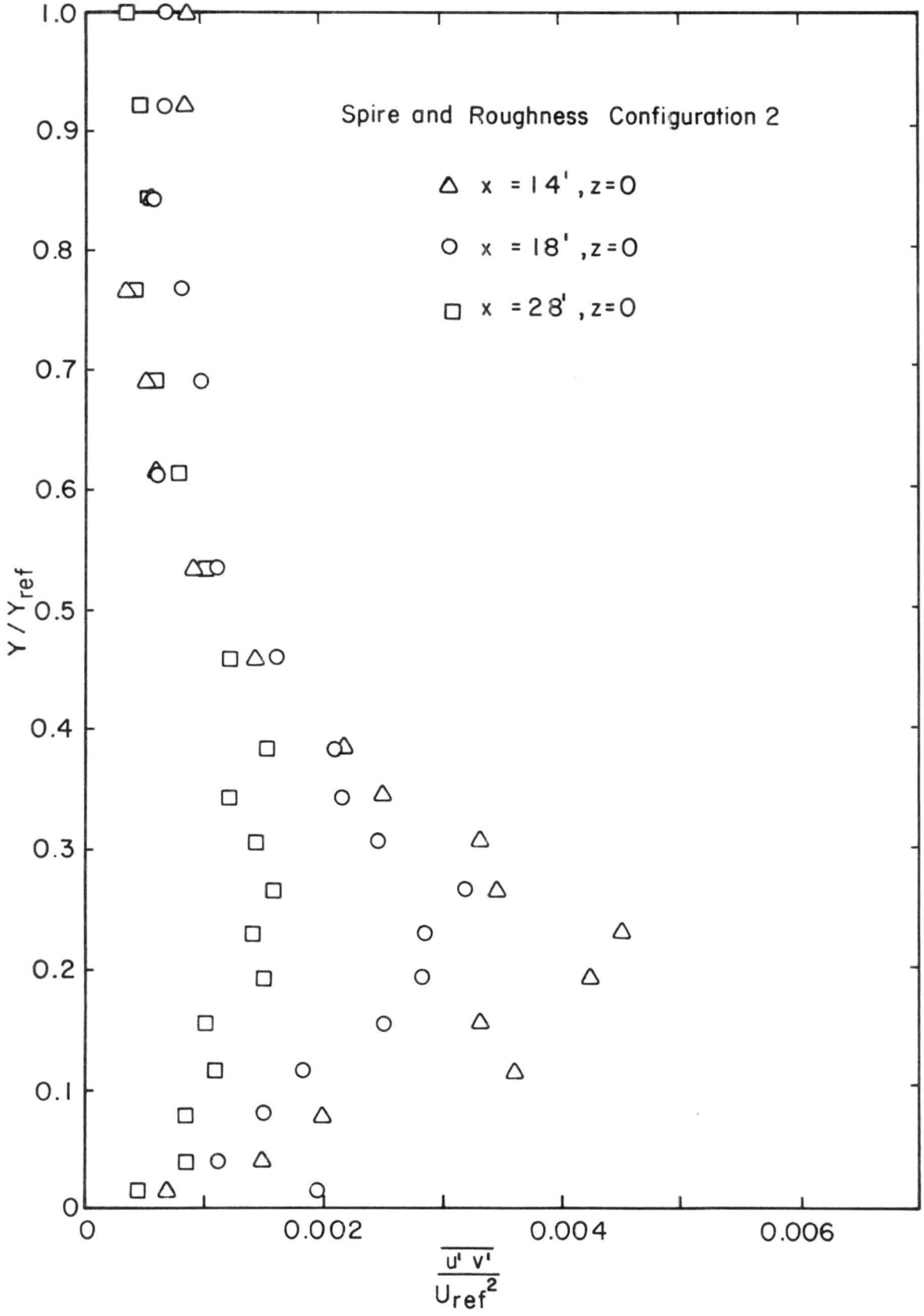

Fig. 15. Shear Stress--Configuration 2 (continued)

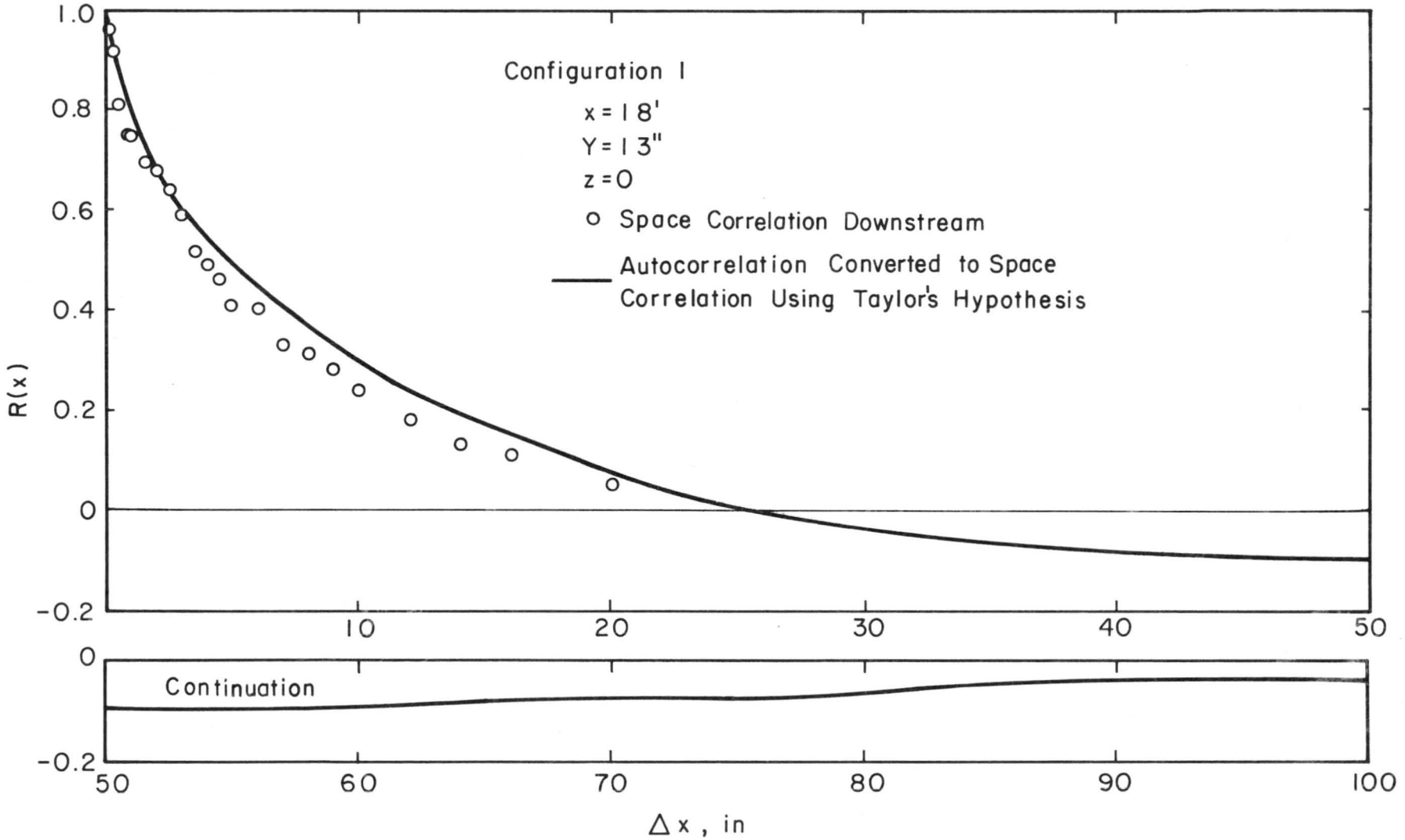

Fig. 16. Longitudinal Space Correlation

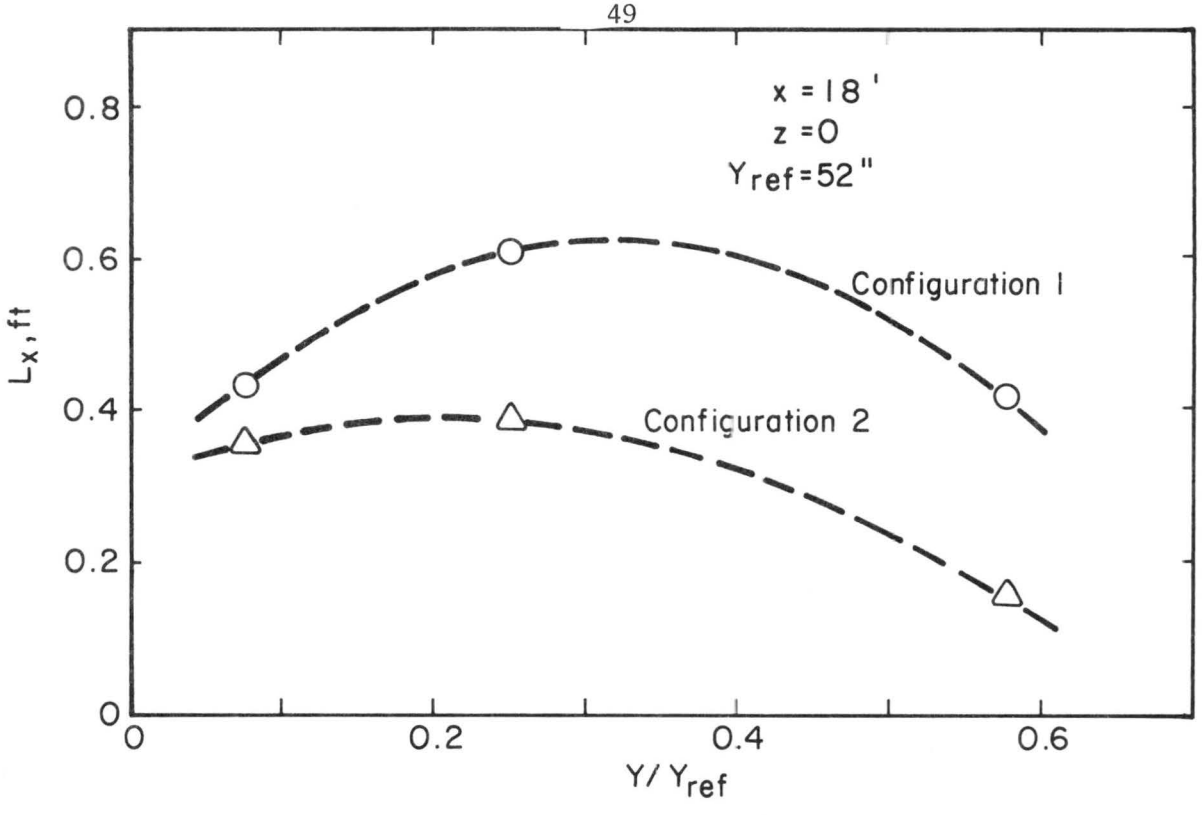

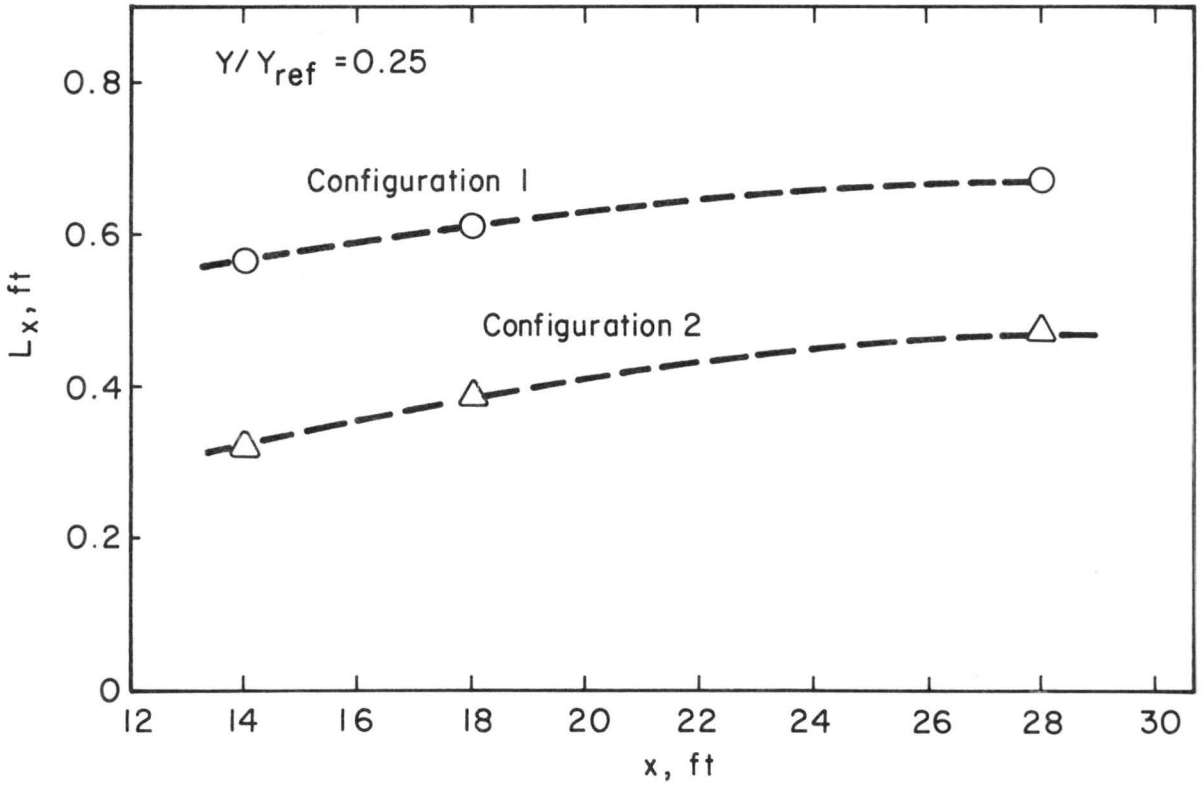

Fig. 17. Integral Scales

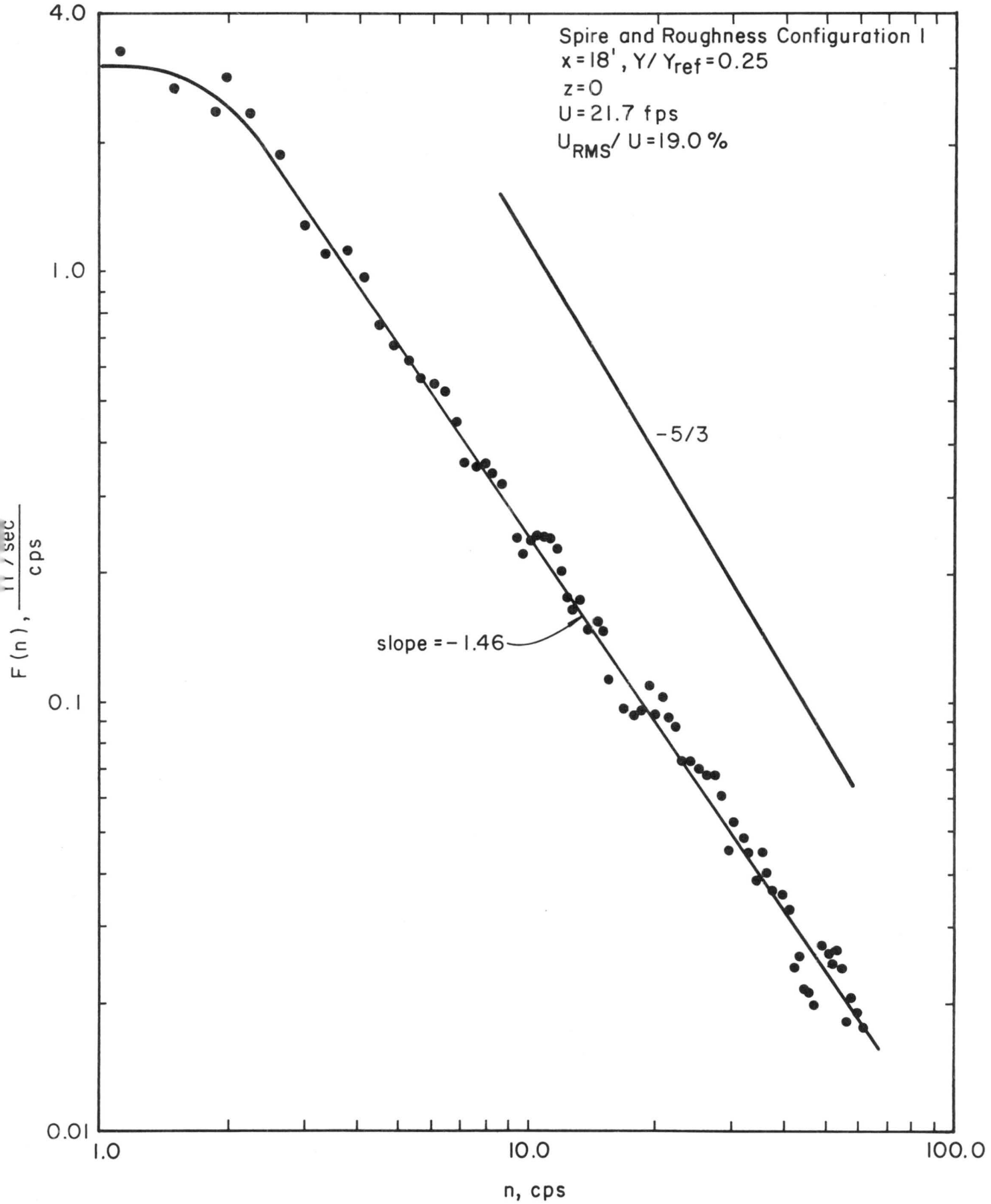

Fig. 18. Velocity Spectra

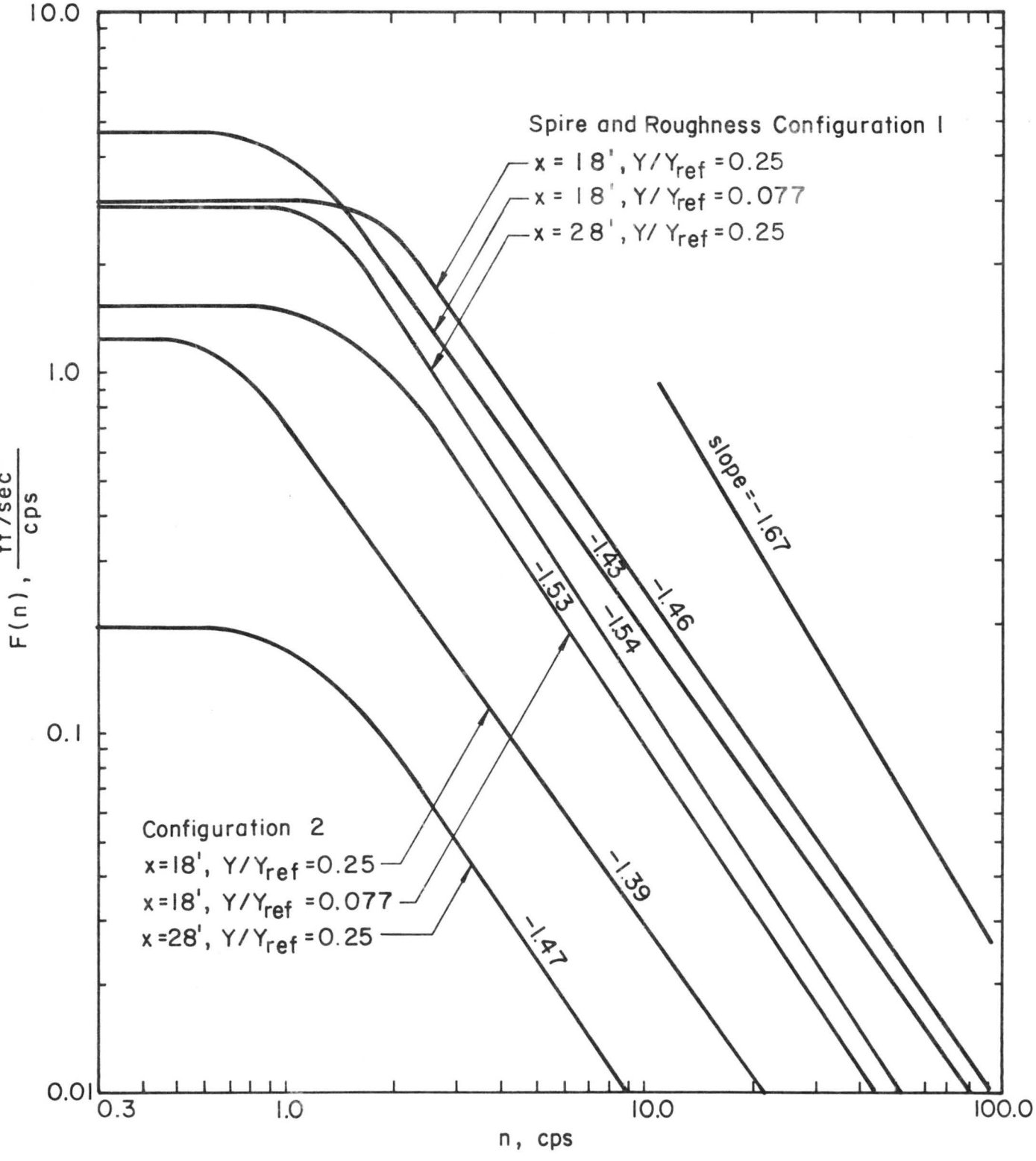

Fig. 18. Velocity Spectra (continued)

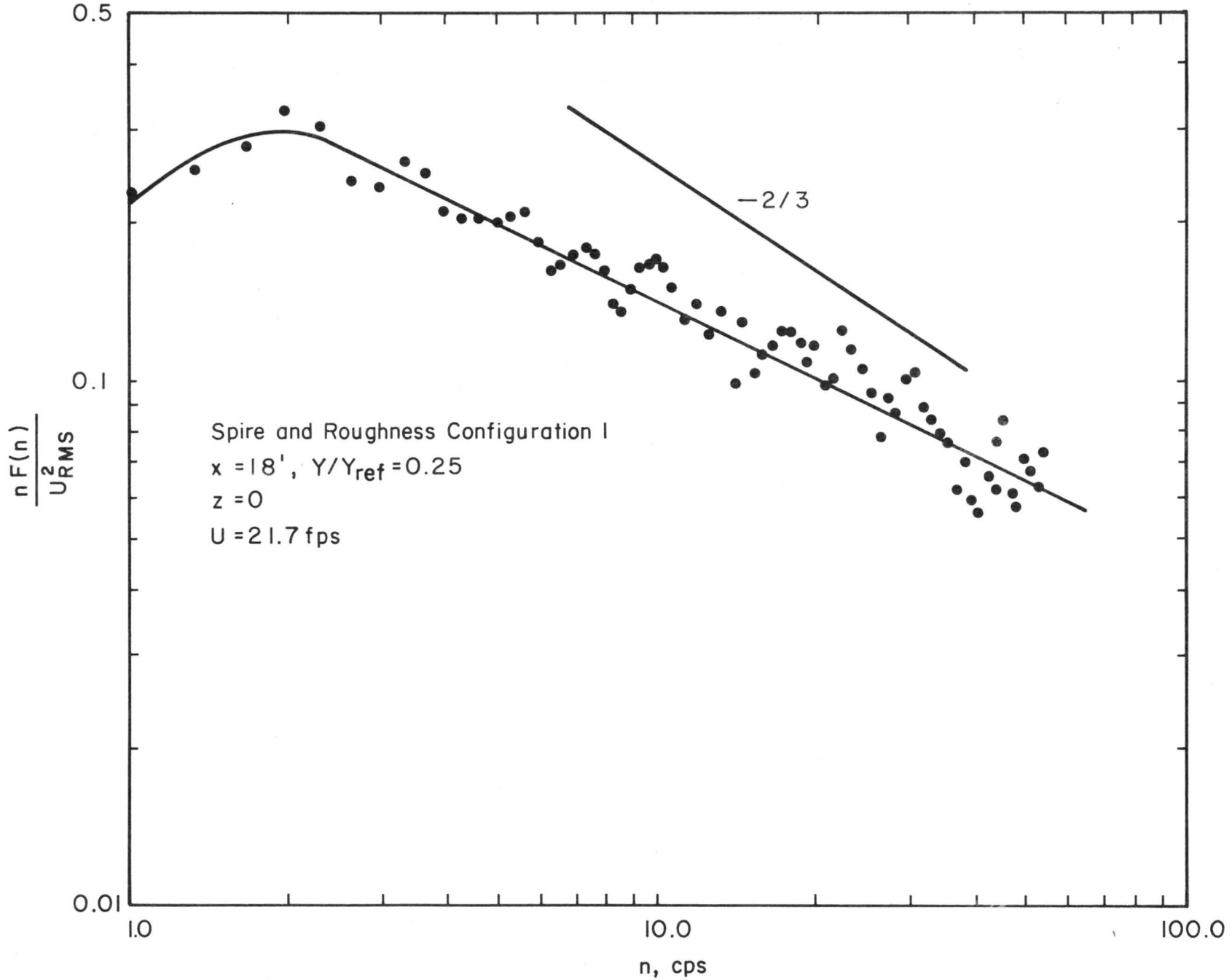

Fig. 19. Normalized Velocity Spectrum